AD NUMBER
AD007924
CLASSIFICATION CHANGES
TO: unclassified
FROM: restricted
LIMITATION CHANGES
TO: Approved for public release, distribution unlimited
FROM: Distribution authorized to U.S. Gov't. agencies and their contractors; Administrative/Operational Use; 15 JUL 1952. Other requests shall be referred to Wright Air Development Center, Wright-Patterson AFB, OH 45433.
AUTHORITY
E.O. 10501 5 Nov 1953; AFRL ltr, 5 May 1972

AD-

7924

RESTRICTED

RESTRICTED

24 July 1952

To: Commanding General
Wright Air Development Center
Wright-Patterson Air Force Base
Dayton, Ohio

Attention: AF 909 30, WPAFB, Service Area
Building 258, Dayton, Ohio
Dept. 31, WCRR

From: Aerophysics Development Corporation

Subject: AF Contract 33(616)-37, Research on Pulse Jet Engines, Quarterly Progress Report

Enclosure: (A) Quarterly Progress Report on Pulse-Jet-Jet, dated 24 July 1952. One reproducible copy and four copies.

1. Enclosure (A) is forwarded herewith in accordance with the requirements of subject contract for submission of quarterly progress reports.

2. The report has been classified "Restricted" due to the use of the information from a restricted report (Reference 9 of Subject Progress Report).

M. E. Stevens
Administrative Engineer
AEROPHYSICS DEVELOPMENT CORPORATION

MES:WW

Copies to: ✓L.A. Regional Office, USAF
Western Air Procurement Dist.
155 West Washington Blvd.
Los Angeles 54, Calif.
Attn: Mr. R. C. Lyon, Cont. Ofcr.

Headquarters
Wright Air Development Center
Area B, Building 56
Wright-Patterson AFB
Dayton, Ohio
Attn: WCUKC

SECURITY INFORMATION

RESTRICTED

AEROPHYSICS DEVELOPMENT CORPORATION

Pacific Palisades, Calif.

Date: 24 July 1952

Report Number: ADC - 102 - 2

Quarterly Progress Report

Preliminary Performance Analysis of the Pulse - Detonation - Jet Engine System

Prepared by: D. Bitondo

Approved by: W. Bollay

SECURITY INFORMATION

PRELIMINARY PERFORMANCE ANALYSIS OF THE PULSE-DETONATION-JET ENGINE SYSTEM

24 July 1952

FOREWORD

This report was prepared by the Aerophysics Development Corporation under U.S. Air Force Contract Number AF 33(616)-37. This is the second quarterly progress report of the work completed by 15 July 1952 under the research and development contract identified by Expenditure Order No. R-467-4 BR-1. The report is the second of a series to be issued on this project, the first having been published on April 1, 1952, the third due on October 24, 1952, and the last and final report due on January 24, 1953.

Included among those who cooperated in these preliminary studies is J. Beggs, who worked on the preliminary design and preliminary layouts of the engine.

CONTENTS

ILLUSTRATIONS

CONTENTS

ABSTRACT

In order to carry out a realistic performance analysis of the pulse-det-jet system, the configuration shown in Figure 1 was assumed. The detonation tubes are arranged in 6 concentric rows of 32 tubes each, giving an engine diameter of 34 inches. The length of the tubes is 15 inches and the overall length of the engine is 55 inches. The dry weight is about 900 lbs.

In order for the engine to operate at the maximum cycle temperature of 3500°F, the most suitable structure was found to be an uncooled tube assembly constructed of suitable high temperature materials. A number of alternate systems, including cooling, were explored. It was found that air cooling requires an abnormally large amount of fin area on the outside of the tubes; liquid cooling requires a large radiator. Zirconium Boride or Graphite promise to be the most suitable materials for uncooled tube structures. Calculations indicate that they are sufficiently thermal shock resistant for the operating conditions of the engine. Graphite coated with molybdenum disilicide or silicon carbide, to prevent oxidation, is commercially available. Zirconium Boride is being made on a laboratory scale and has shown outstanding performance in small rocket nozzles.

The experimental apparatus for initiating a detonation wave by means of a shock wave has been set up and some preliminary experiments have been initiated.

This engine configuration shows its greatest promise as a competitor to the ram-jet. It can deliver as much thrust as the ram-jet at the higher Mach Numbers at a lower specific fuel consumption and, at the same time, provide static thrust and power to accelerate from take-off to high supersonic cruising speed.

INTRODUCTION

The first quarterly progress report (Reference 1) gave the preliminary performance for the simplified cycle of the Pulse-Det-Jet. Relations for the specific fuel consumption, thrust per unit area, and pounds of thrust per pound of air per second have been calculated for subsonic flight Mach Numbers over a wide range of pressures and temperatures. A second series of computations was carried out, including the inlet and duct frictional losses. The performance was computed and plotted against the following parameters:

(a) $\frac{L}{D}$ - length/diameter ratios

(b) M_o - flight Mach Number

(c) M_d - duct Mach Number

(d) T_7 - maximum cycle temperature

These first computations determined some of the critical elements of the propulsion system. They are:

(1) The initiation of detonation

(2) The design of the valve and timing mechanism

(3) Grouping of tubes in one unit

(4) Estimation of burning time

(5) Estimation of valve opening and closing times.

The work reported herein is a continuation of the research reported in Reference 1.

SECTION I

PRELIMINARY ANALYSIS OF AN ENGINE CONFIGURATION

1.1 Applications of the Engine

The application of the engine will determine its actual form and performance. It is felt that the applications of this engine will be many and varied. In order to simplify the preliminary performance estimation, a specific type was considered. This permitted an analysis of the valve configuration, the valve characteristics, and the effect of the valve on the performance.

Promising applications of this engine appear to be as follows:

1. Power Pack
2. Guided Missile Power Plant with Static Thrust
   (a) Subsonic
   (b) Supersonic
3. Aircraft Powerplant
   (a) Subsonic
   (b) Supersonic
4. Helicopter Propulsion
5. Combustion Chamber or Afterburner for a Turbo-Jet
6. Burner for a Ram-Jet
7. Stationary Engine as an Auxiliary Power Plant

It was decided to consider an engine capable of propelling a guided missile from zero flight speed to a cruising Mach Number of 2.80. The choice of these flight speeds does not preclude that these are the limits, but only sets down a definite application for the Pulse-Jet-Jet. For any other application, the configuration will have to be modified to suit the requirements.

1.2 Preliminary Design Layouts

The mechanical design layouts of a typical engine embodying the pulse detonation cycle had to be considered in order to determine that there were no obvious mechanical problems that could not be solved. The mechanical design was not considered in detail, but only generally. This was also necessary so that more realistic valve characteristics could be calculated. The mechanical grouping of the tubes was also a governing factor affecting the efficiency of the discharge and scavenging phases. As is shown in Section III, these preliminary design considerations have indicated that the heat transfer problem in the cooling of the tubes and the whole engine is a major one for an engine of high specific thrust, and that the most promising solution is to construct the tubes from ceramic materials or coated graphite.

DIMENSIONS..

OVERALL LENGTH . 55"
MAX. DIAM... 34"
DRY WEIGHT... 900 lbs.
MAX. VALVE ROTATIONAL SPEED
AT SEA LEVEL... 3900 R.P.M.

PERFORMANCE.. (M_{MAX} AT SEA LEVEL = 1.16) (T_{MAX} = 3500° F)

	STATIC (SEA LEVEL)	M = 1.16 SEA LEVEL	M = 2.80 30,000 FT. ALTITUDE
THRUST (LBS.)	4300	9500	9000
SPECIFIC FUEL CONSUMPTION $\frac{\text{LBS FUEL/HOUR}}{\text{LB. THRUST}}$	1.45	1.52	1.56
$\frac{\text{THRUST (LBS.)}}{\text{SQ. FT. FRONTAL AREA}}$	681	1500	1430
THRUST COEFFICIENT	—	0.96	0.53
$\frac{\text{THRUST (LBS.)}}{\text{LB AIR/SEC}}$	116	106	62.5

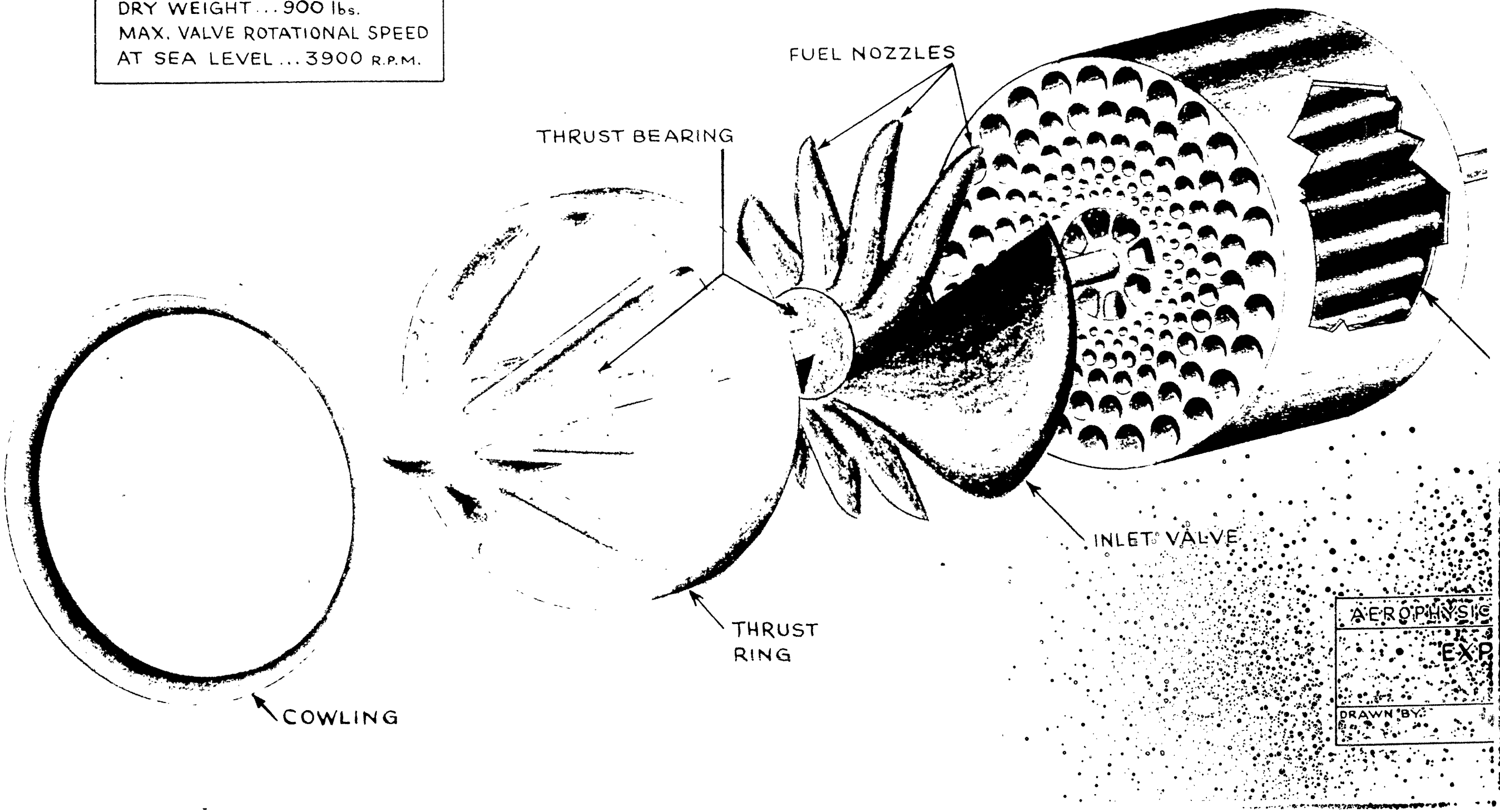

AEROPHYSIC
EXP
DRAWN BY

FIG. 1

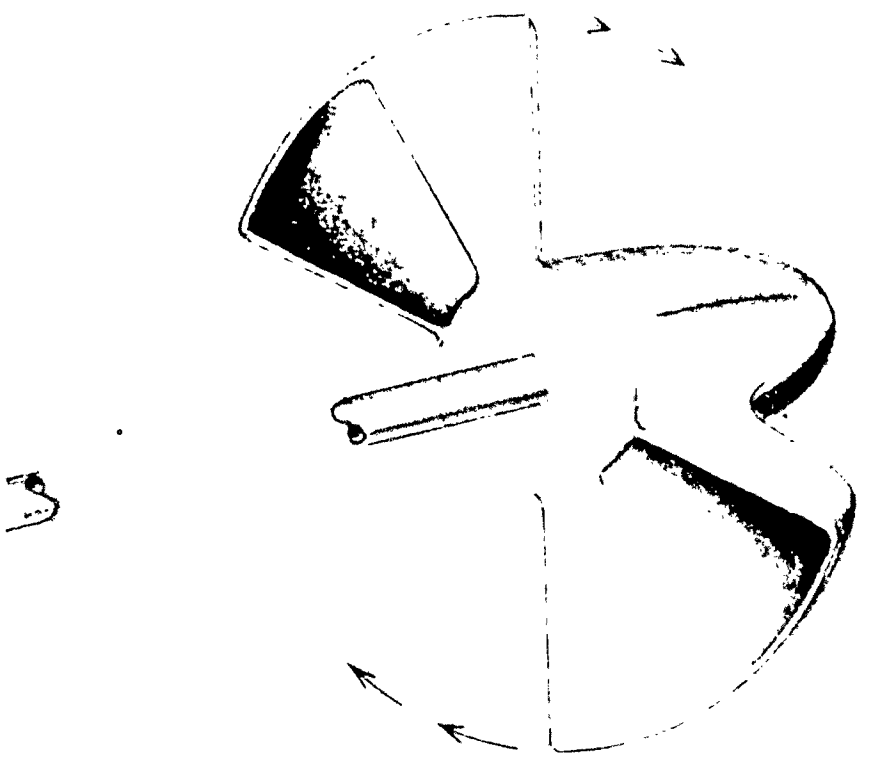

S DEVELOPMENT CORP. Pacific Palisades, Calif.

LODED VIEW OF PULSE-DET-JET

DATE:

Consideration on the preliminary design layouts went along hand-in-hand with the preliminary performance calculations. Many designs were considered for the valves, including flap, butterfly, venetian blind, sleeve and rotating plate types. At first it was decided that each individual tube have its own valve. This would be necessary when the tube is used to power a helicopter rotor, but when a number of tubes are nested in a group, the mechanism of operating and timing each single valve becomes too cumbersome and complicated.

It has been noted (Reference 1) that short closing and opening times are required and therefore vibratory motions were considered for the valves. On the other hand, the large accelerations required for opening and closing necessitated the use of very heavy and cumbersome springs. The rotating sleeve-type valve on a single tube with inlet and discharge openings arranged in slots on the tube wall required high rotational speeds and presented too large a bearing surface.

The drum type valve with the tubes arranged around its periphery and discharging through slots perpendicular to the tube axes showed the most promise. This configuration was soon discarded due to its inherent disadvantage of limiting the arrangement of the tubes to one row. The ratio of the total cross sectional area of the tubes to the maximum cross sectional area of the engine was too small (i.e. 26%).

This led to a second design configuration (See Figure 1), where the air flowed straight through the tubes and each valve took the form of a rotating disc with cutouts. With this arrangement, up to 60% of the maximum cross sectional area of the engine could be utilized as combustion chamber area.

The maximum tip speed of the rotating valves was set at 750 ft/sec. The cutouts in the valves were arranged so that diametrically opposite tubes were discharging at the same time, producing a force balance about the center line of the engine. Each tube cycles twice for each revolution of the valve. This determines the length of the tubes to be 15 inches. The diameters of the tubes were kept as small as possible in order to keep the cut-off times as short as possible.

The speed of the valve and the number of cycles for each valve revolution determines the duration of a cycle. The duration of a cycle determines the length of the detonation tubes. For a two-cycle valve (each tube cycles twice for each valve revolution) and a given tube length, the angle subtended by each tube determines the time required for the tube to open and to close. The ratio of the time the tube is opening and closing to the time the tube is fully opened determines the amount of air that actually flows into the tube.

Case (a) The lower limit of the tube lengths, for an engine with a two-cycle valve with an upper limit of 750 fps on the valve tip speed, is 15 inches.

This tube length can only be reduced by having the tubes cycle more than twice for each valve revolution. Since a force balance is necessary about the center line of the engine, only an even number of cycles per valve revolution can be used.

Case (b) The lower limit of the tube lengths, for an engine with a four-cycle valve with an upper limit of 750 fps on the valve tip speed, is 7½ inches.

For Case (a) the ratio of the time the valve is fully open to the total time the valve is opened is 0.770; for Case (b) the ratio is 0.59. The mass flow for Case (a) is 88.5% of the mass flow of a theoretical engine having valves that open and close discontinuously. The mass flow for Case (b) is 79.5% of that of the theoretical engine. The thrust of the engine of Case (b) is 89% of that of the engine operating under the conditions of Case (a). The engine weight of Case (b) is only 89% of the weight of the engine of Case (a). Since only a very slight gain is obtained in thrust/weight ratio by using the 7½-inch tubes, the requirement of having the larger thrust from the 15-inch tubes becomes more important. For maximum thrust, 15 inches is the optimum length for the tubes of this engine. On the other hand, it may be practical to air cool the shorter tubes and for other applications this may be a determining factor.

Preliminary heat transfer calculations show that approximately eight times the surface area is required for fins on the outside of each tube to cool the wall to 1500° F when the maximum cycle temperature is 3500° F. This leads to a very heavy construction for each tube, and it also necessitates moving the tubes farther apart, giving a poor nesting arrangement. Liquid cooling required a very large radiator and a large mass flow of liquid. It was decided, therefore, to consider ceramic materials for the tubes, such as stabilized zirconium oxide or graphitar. Section III gives a complete discussion on the cooling problem. The allowable maximum pressure level in the tubes, based on stress considerations, will determine the maximum Mach number for each altitude.

The valves, on the other hand, must be cooled and, since the fuel must be heated in order for it to vaporize on injection into the air, fuel cooling is used on the valves. The fuel will be brought into a header at the front of the engine, where it will be allowed to flow spirally around, and towards the rear of the engine. It then will be ducted through struts to the

axial shaft, then into the rear valve. It will then flow forward through the shaft into the front valve and then to the fuel nozzles. The pressure in the fuel system will be such that the fuel will remain in the liquid form throughout its passage. As soon as the pressure of the fuel is reduced upon its injection into the air stream, the fuel will vaporize. Vaporized fuel will be necessary to support detonation.

The source of power with which the valves are to be driven has not been definitely decided upon. The following methods have been considered:

1. Turbine driven by some of the exhaust gases
2. Turbine driven by the inlet gases
3. Auxiliary turbine driven by a gas generator
4. Auxiliary powerplant

The method finally selected will be determined partially by the system used to govern the speed of valves. It will be necessary to control the valve speed reasonably accurately. The calculations so far have indicated that the valve speed is a function of the square root of the inlet total temperature.

The solid portion of the exhaust valve is hollowed out to permit the feed-back of the high pressure and temperature gases. The duct in the exhaust valve is positioned such that it interconnects the tubes which are at a high pressure to the tubes that are ready to be ignited. In this way, a very strong shock wave is formed and propogated through the fuel-air mixture. Spot calculations show that a pressure ratio of about 4 to 5 can be obtained across the shock wave with this cross-feed. This cycle will be investigated and reported in the next progress report.

Figure 1 shows an artist's conception of the engine exploded to the main sub-assemblies.

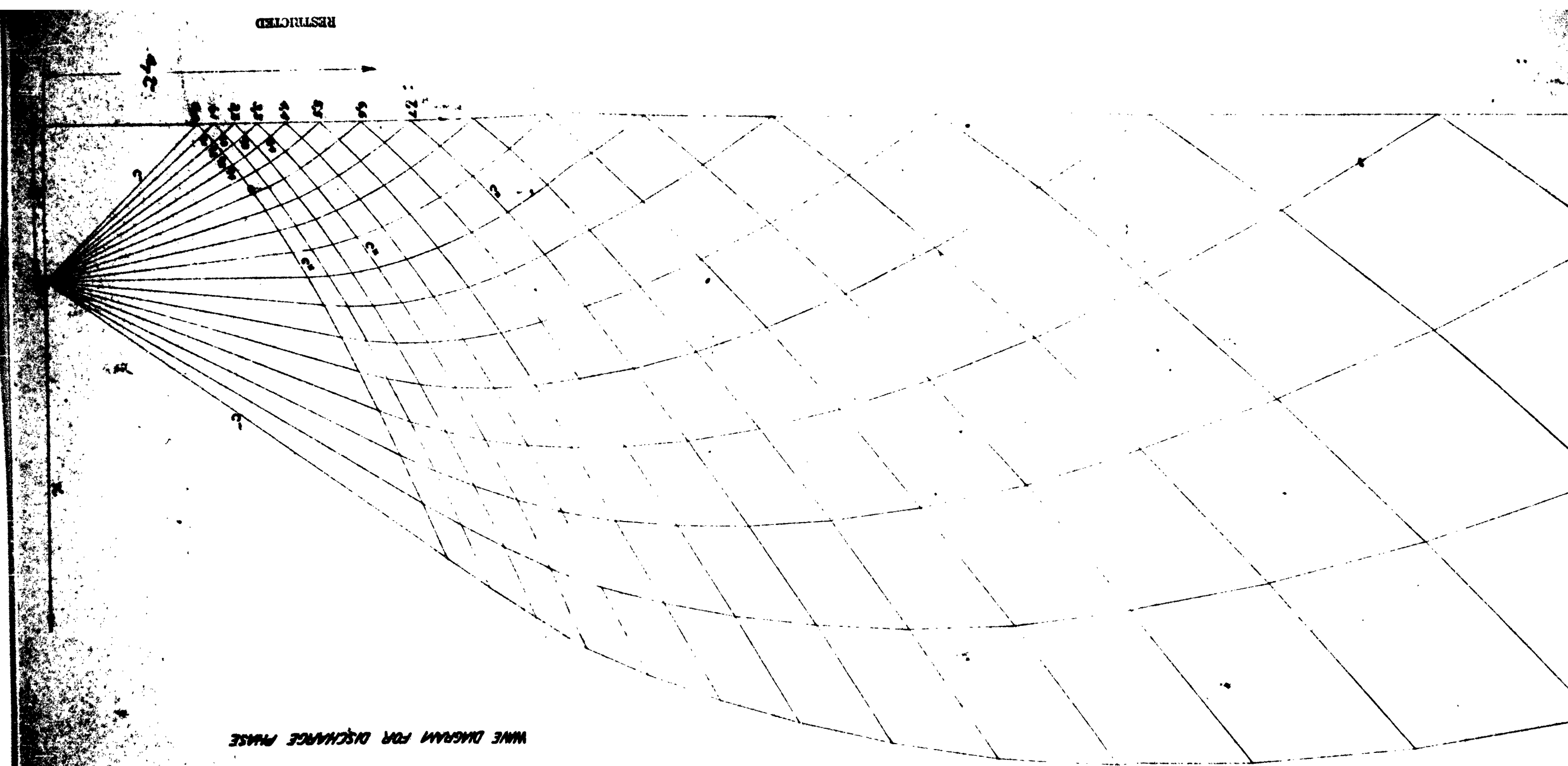

WAVE DIAGRAM FOR DISCHARGE PHASE

SECTION II

PERFORMANCE ANALYSIS OF PRESENT CONFIGURATION

2.1 Cycle of Operation

The basic cycle was described in the previous progress letter (Reference 1). The actual cycle of operation is only slightly modified due to finite cut-off times. Figure 5 shows the wave diagram on a time-distance plot. The pressure in the tube is allowed to drop during the discharge phase to a predetermined value, less than the inlet ram pressure. When the inlet valve opens (start of scavenging) a compression wave is formed which travels down the tube accelerating the burnt gases to the required Mach Number. The fresh fuel-air mixture is admitted at the front end, while the burnt mixture is ejected axially out the back.

The shock wave produced during the pulse compression phase will be used to ignite or detonate the fuel air mixture. Actually, this wave is relatively weak (pressure ratio $\approx$ 2.0) and therefore an easily detonable fuel will have to be injected into the front end of the tubes, while the remainder will contain the regular fuel. An alternate method of detonating the fuel is at present being studied, but the cycle calculations have not yet been completed. Briefly, this method uses the hot high pressure gases from a tube that has been previously fired and ducts them back through the exhaust valve into a tube which is ready to be fired. This produces a very strong shock (pressure ratio $\approx$ 4 or 5) and also produces a much higher maximum cycle pressure. However, this full pressure is not realized for the discharge, since the gases are fed back to ignite another tube. The first preliminary calculations show that the thrust is not changed from the basic cycle and the specific fuel consumption is only slightly increased, but the advantage gained by having a strong shock present makes this type of cycle preferable over the basic cycle described previously. Further investigations of this cycle are being continued.

2.2 Non-Stationary Flow Process During the Discharge Phase

Simplified investigations were carried out on the non-stationary flow process to determine the actual duration of a cycle for given inlet conditions.

The following assumptions were made in order to compute the wave diagram for the discharge phase:

1. The exhaust valve is opened instantly
2. One-dimensional flow is considered only (Straight duct fore and aft of exhaust valve)

The procedure followed for the calculations was that given by Guderley in Reference 2. The wave diagram is shown in Figure 2.

Along the C^+ characteristics

$$\frac{dx}{d\,a_7 t} = \frac{u}{a_7} + \frac{a}{a_7} \qquad \text{----------(1)}$$

$$\frac{2}{\gamma-1}\left(\frac{a}{a_7} - 1\right) + \frac{u}{a_7} = \lambda = \text{CONSTANT} \qquad \text{----------(2)}$$

Along the C^- characteristics

$$\frac{dx}{d\,a_7 t} = \frac{u}{a_7} - \frac{a}{a_7} \qquad \text{----------(3)}$$

$$\frac{2}{\gamma-1}\left(\frac{a}{a_7} - 1\right) - \frac{u}{a_7} = \mu = \text{CONSTANT} \qquad \text{----------(4)}$$

where a = velocity of sound

u = particle velocity

and the conditions in state (7) are those existing in the tube just before the exhaust valve is opened.

By the use of the above equations, the values for λ and μ can be found for each point on the characteristic net.

The inlet valve (which is closed) is located at position A; the exhaust valve (which is opened) is located at position B. (See Figure 2). Along the inlet valve the C^- characteristics are reflected and they become the C^+ characteristics and therefore $\lambda = \mu$ at the inlet valve. For any state (i), solving the previous equations, we get

$$\frac{a_i}{a_7} = \left[\frac{\lambda + \mu}{4}(\gamma-1) + 1\right] \qquad \text{----------(5)}$$

$$\text{but} \quad \frac{P_i}{P_7} = \left(\frac{a_i}{a_7}\right)^{\frac{2\gamma}{\gamma-1}} \qquad \text{----------(6)}$$

and $\lambda = \mu$, $\gamma = \frac{9}{7}$ in our case

$$\therefore \quad \frac{P_i}{P_7} = \left[\frac{\gamma}{2}(\gamma-1) + 1\right]^{\frac{2\gamma}{\gamma-1}} \qquad \text{----------(7)}$$

AEROPHYSICS DEVELOPMENT CORP.
REPORT NO ADC-102-2
FIGURE 3

TOTAL PRESSURE DURING DISCHARGE

INDEX POINT	μ	P_t/P_T
0, 0	0	1.000
1, 1	-.175	.796
2, 2	-.350	.631
3, 3	-.525	.496
4, 4	-.700	.388
5, 5	-.875	.301
6, 6	-1.050	.232
7, 7	-1.225	.177
8, 8	-1.400	.135
9, 9	-1.575	.101
10, 10	-1.750	.0755
11, 11	-1.925	.0555
12, 12	-2.100	.0406
13, 13	-2.275	.0293
14, 14	-2.450	.0207
15, 15	-2.625	.0148
16, 16	-2.800	.0102
17, 17	-2.975	.0069

Figure 3 gives the value of μ , p_1/p_2 for each point of reflection. The numbering on each point on the characteristic net is arbitrary.

For given conditions in the combustion chamber just prior to the discharge phase and for a given pressure at the inlet valve, the time required for discharge down to this pressure can be found from Figures 2 and 3. The distance A B is scaled off to equal the length of the combustion tube. Using the same scale, the distance from the origin to the correct index point measured along the time axis is found. This number is then divided by a_7 (using consistent units) to give the time required for the pressure to drop from P_7 to P_1 at the inlet valve. The time obtained for the discharge phase in this manner checks to within 1% of the time computed by steady flow methods.

Typical case for $k_0 = 2.00$ $T_7 = 3960^\circ$ R
$a_7 = 2955$ ft/sec $p_1/p_7 = 0.0907$

τ Disch. (Steady) = 0.00157 secs.
$\mu = 1.64$ τ Disch. (non-stat.) = 0.00156 secs.

The pressure at the end of the discharge phase will be determined by the flow velocity required for scavenging. It will be assumed that the inlet valve opens instantaneously. The pressure ratio across the inlet valve will be such that when the valve opens a wave configuration is formed which accelerates the new fuel-air mixture to $M_2 = 0.6$. The pressure in front of the valve is the total pressure of the inlet air. (p_{2t}). The wave configuration formed by the opening of the inlet valve is shown on Figure 4. The valve is located at point A. The valve opens at $\tau = 0$. A typical case

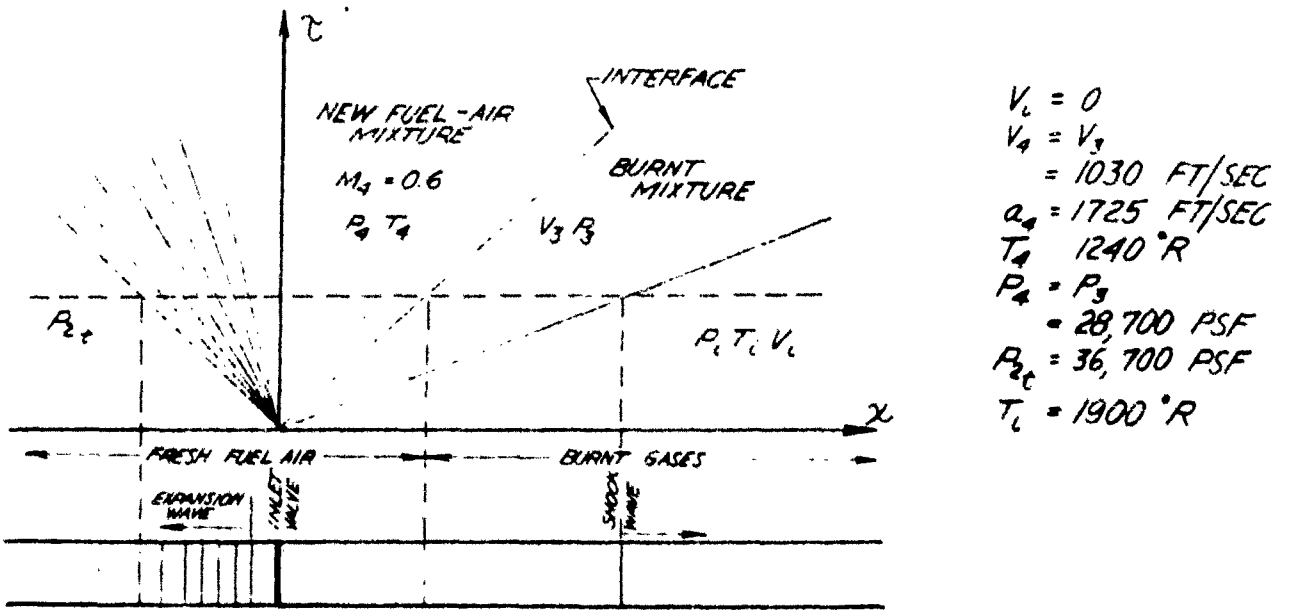

FIG. 4 WAVE CONFIGURATION PRODUCED WHEN INLET VALVE OPENS

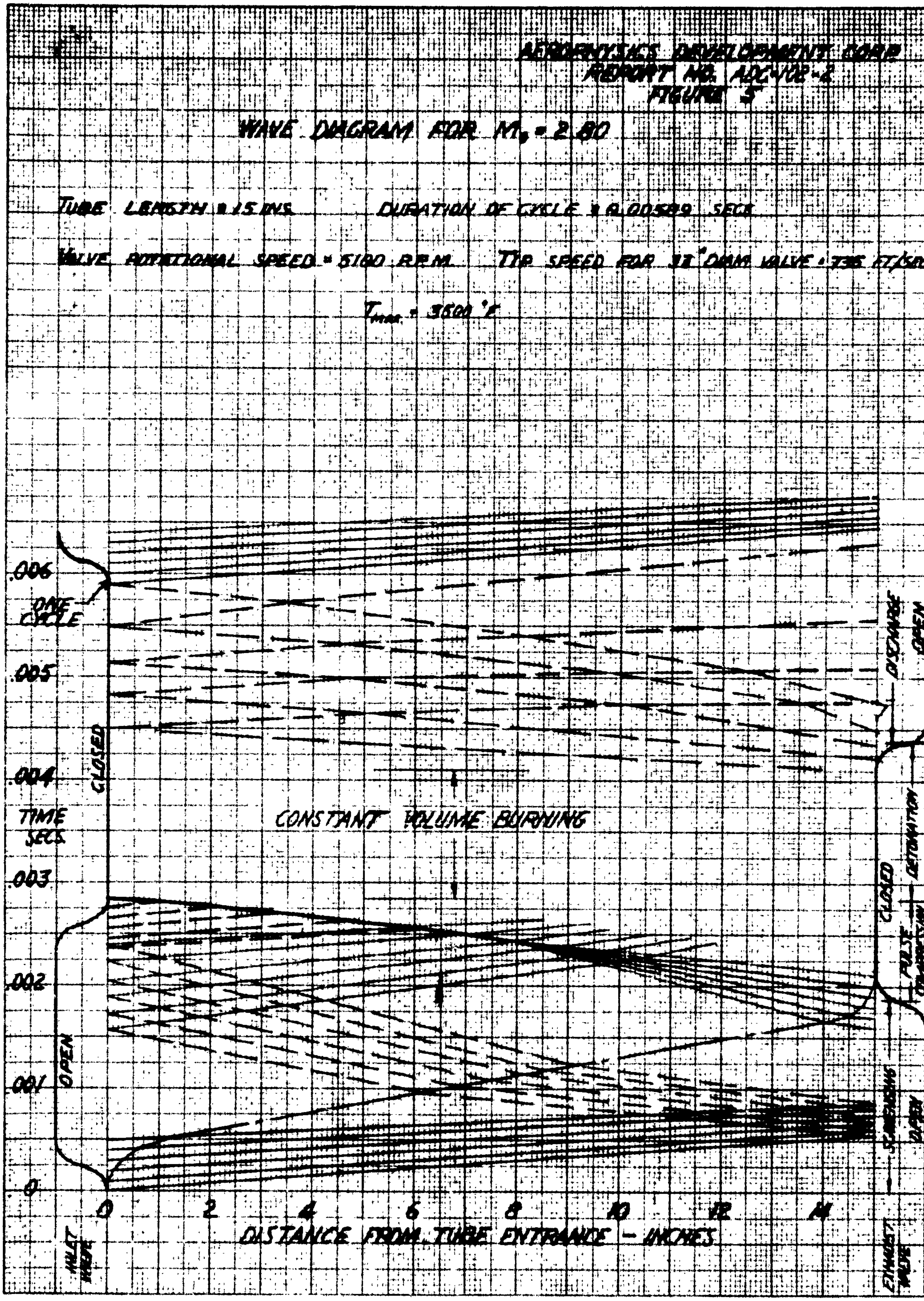
AEROPHYSICS DEVELOPMENT CORP
REPORT NO. ADC-102-2
FIGURE 5
WAVE DIAGRAM FOR M = 2.80
TUBE LENGTH = 15 INS.
DURATION OF CYCLE = 0.00589 SECS
VALVE ROTATIONAL SPEED = 5100 R.P.M.
TIP SPEED FOR 33" DIAM VALVE = 735 FT/SEC
Tmax = 3500 °F
.006
ONE CYCLE
.005
.004
TIME SECS.
.003
.002
.001
0
CLOSED
OPEN
CONSTANT VOLUME BURNING
DISCHARGE OPEN
CLOSED
DETONATION
PULSE COMPRESSION
SCAVENGING
OPEN
0
2
4
6
8
10
12
14
DISTANCE FROM TUBE ENTRANCE - INCHES
INLET VALVE
EXHAUST VALVE

AEROPHYSICS DEVELOPMENT CORP.
REPORT NO. ADC-102-2
FIGURE 6

WAVE DIAGRAM FOR $M_0 = 2.00$

TUBE LENGTH = 15 INS. DURATION OF ONE CYCLE = 0.00681 SECS.

VALVE ROTATIONAL SPEED = 4410 RPM TIP SPEED FOR 33" DIAM. VALVE = 636 FT/SEC

$T_{MAX} = 3500\ ^\circ F$

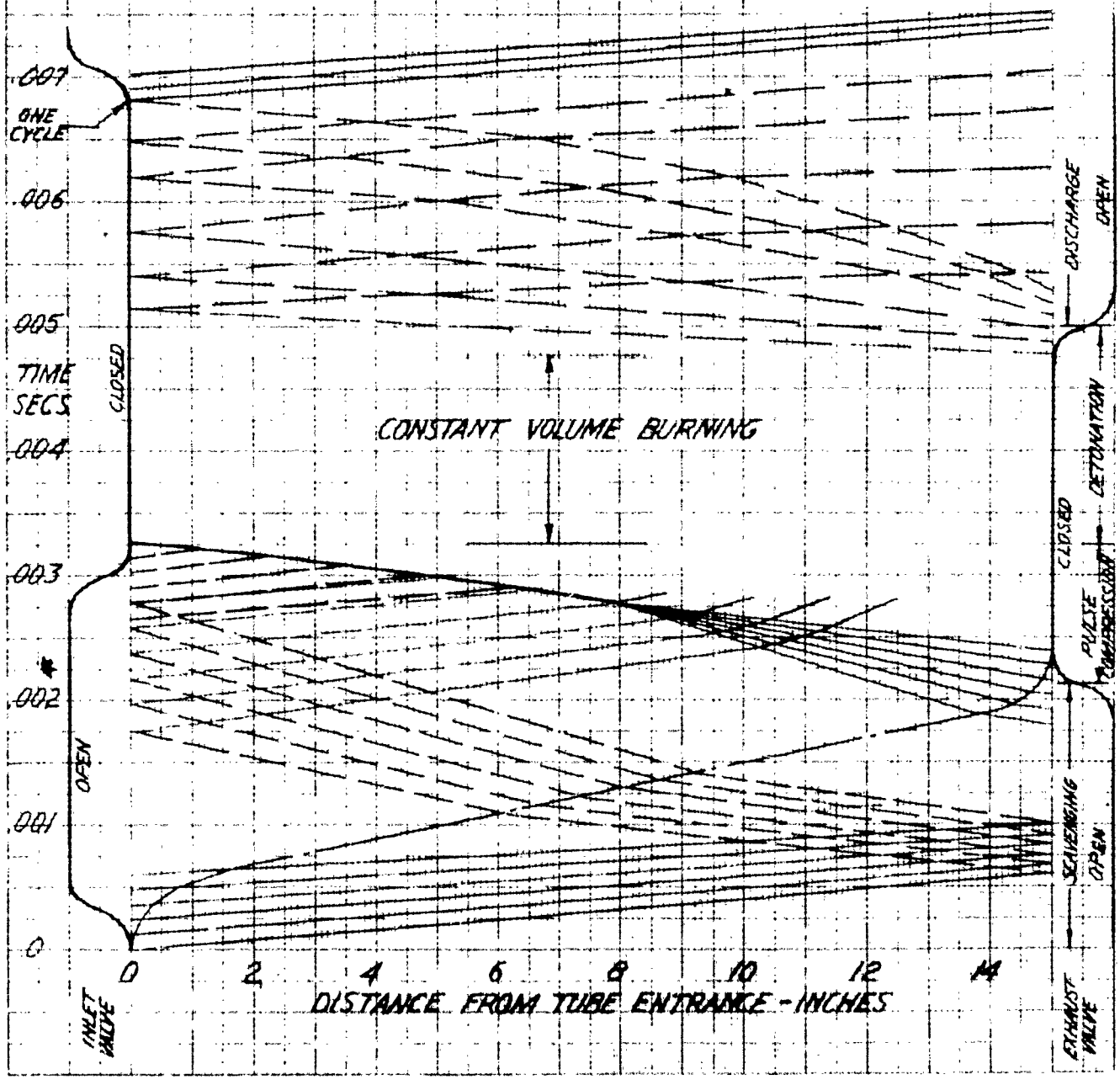

REPORT NO. ADC-102-2 AEROPHYSICS DEVELOPMENT CORP.

FIGURE 7

WAVE DIAGRAM FOR $M_0 = 1.00$

TUBE LENGTH = 15 INCHES DURATION OF ONE CYCLE = 0.0089 SECS.

VALVE ROTATIONAL SPEED = 3680 RPM TIP SPEED FOR 33" DIAM. VALVE = 530 FT/SEC

$T_{MAX} = 3500°F$

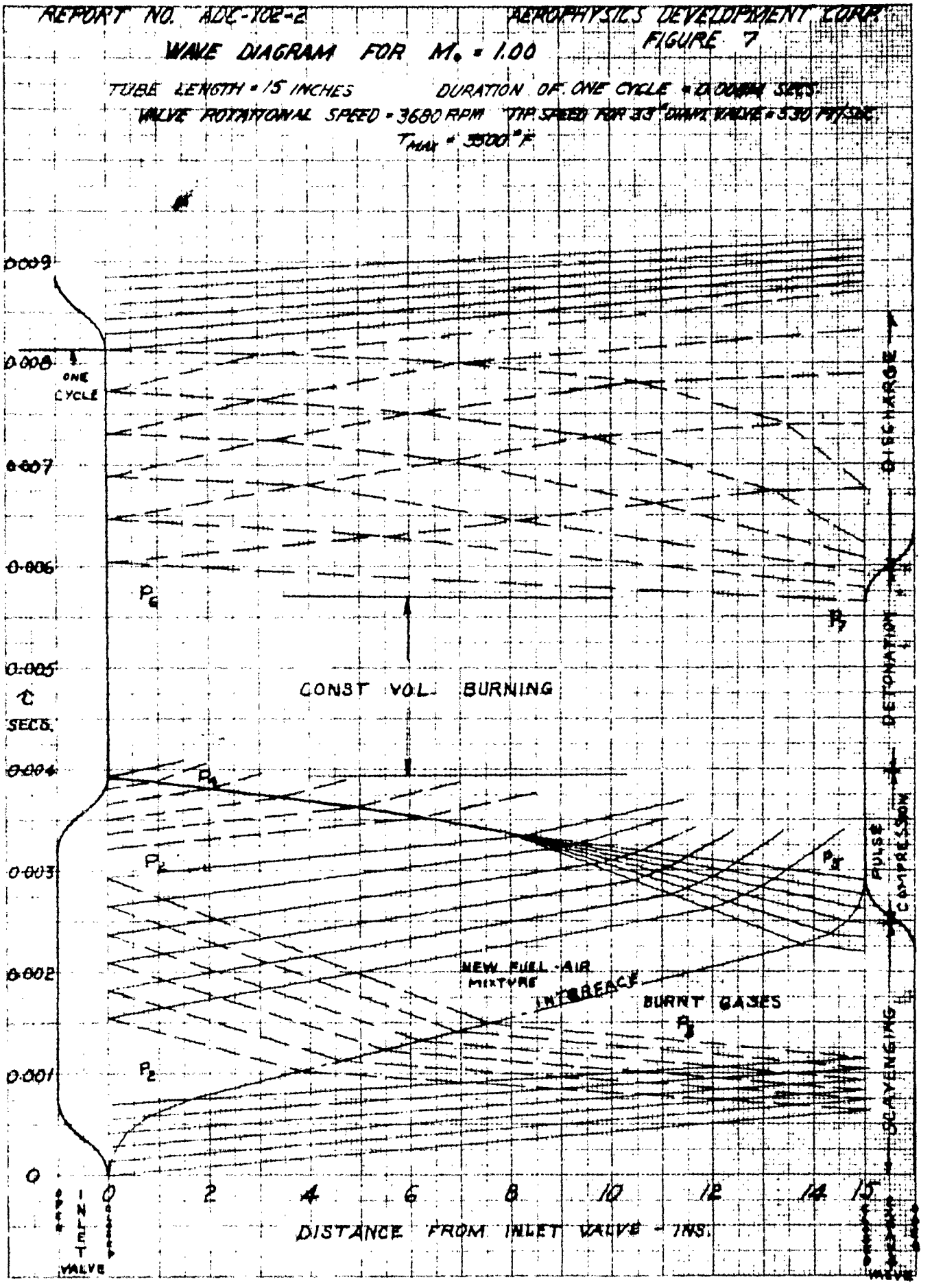

REPORT NO. ADC-102-2 AERO PHYSICS DEVELOPMENT CORP.

WAVE DIAGRAM FOR STATIC CONDITIONS FIGURE 8

TUBE LENGTH = 15 INS. DURATION OF CYCLE = 0.00889 SECS.

VALVE ROTATIONAL SPEED = 3380 R.P.M. TIP SPEED FOR 33" DIAM. VALVE = [illegible] FT/SEC

T_{max} = 3500 °F

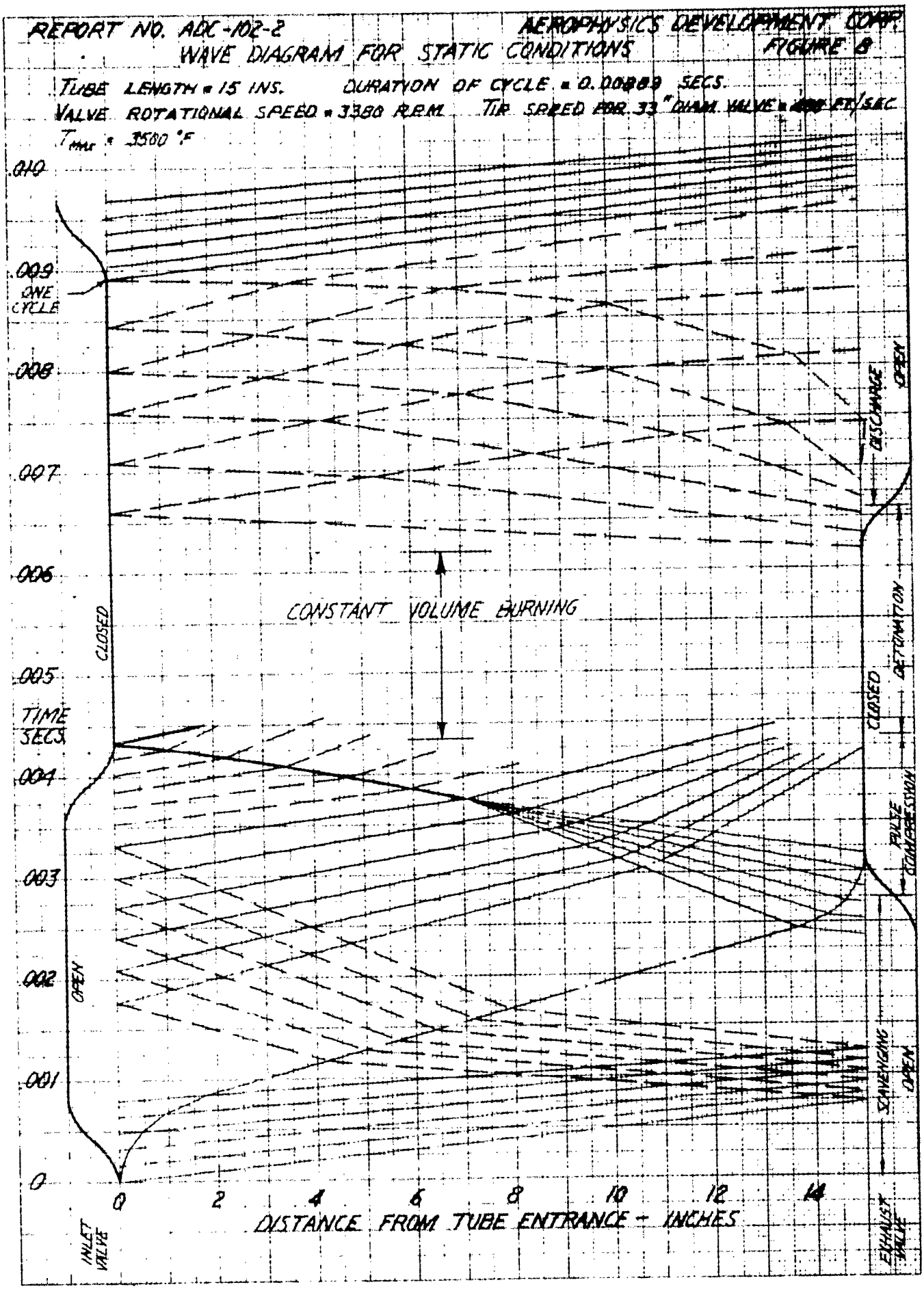

AEROPHYSICS DEVELOPMENT CORP.
REPORT NO. ADC-102-2
FIGURE 9

VALVE TIMING DIAGRAMS

LENGTH OF TUBES = 15"
DIAMETER OF VALVES = 3.3"

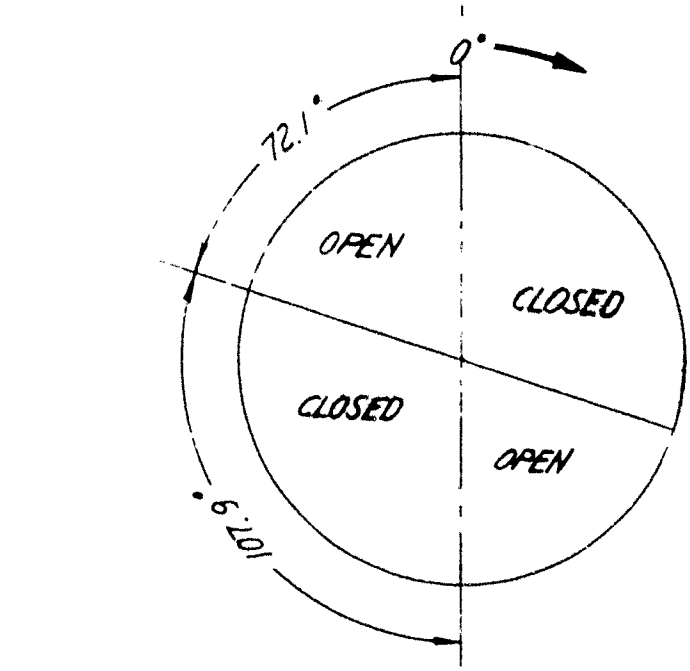

INLET VALVE

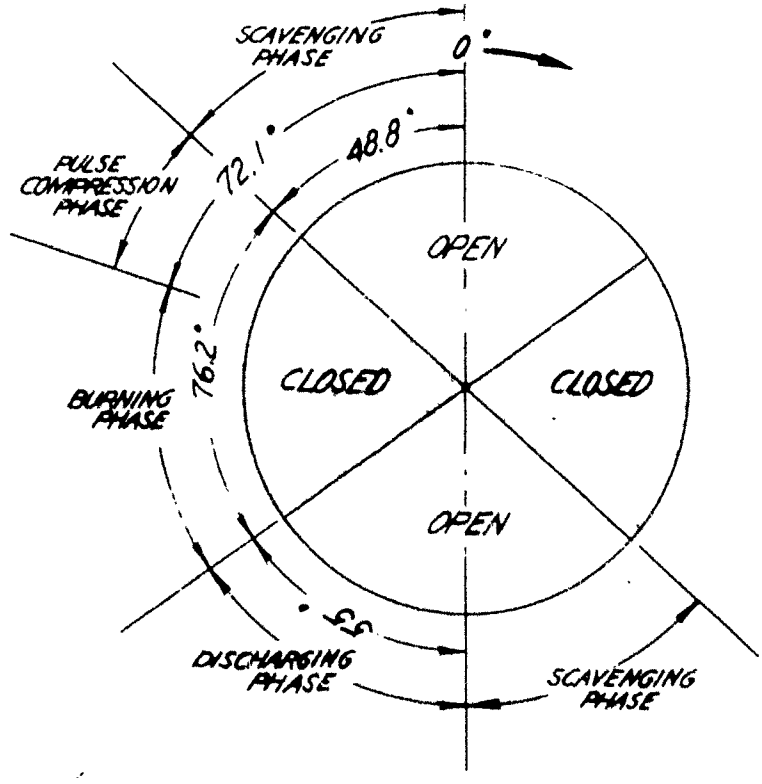

EXHAUST VALVE

is $M_o = 2.80$.

$$V_3 = V_i - \left(\frac{P_3}{P_i} - 1\right) \sqrt{\frac{2 a_i^2}{\gamma\left[(\gamma+1)\frac{P_3}{P_i} + (\gamma-1)\right]}}$$

$$\frac{P_3}{P_i} = 1.70 \qquad \therefore \frac{P_{3r}}{P_i} = 2.17$$

2.3 Wave Diagram for a Cycle

The non-stationary wave diagrams were drawn by using the assumption of linear variations as the valves opened. The acceleration of the interface between the burnt and new mixtures was assumed to take place through a compression wave having a pressure ratio of 1.70. This strength of wave produces a flow Mach Number in the tube of 0.6. The compression wave was divided into five parts (or characteristics), each characteristic increasing the interface velocity by 1/5 of the final velocity to give a final Mach Number of 0.6 in the new mixture. The stopping of the fluid particles and the formation of the shock wave by the exhaust valve is computed in the same way. For these computations and for tubes of 15 inches in length, the time for constant volume burning was assumed to be 0.0015 secs., for $M_o = 2.80$. For any of the other flight Mach Numbers (M_o), the rotational speed of the valve was computed from the scavenging and the pulse compression phases of the cycles. By making the opening and closing times of the valves coincide with the arrival of the waves in these phases, the duration of the total cycle was obtained. This automatically determined τ_{BURN} and $\tau_{DISCH.}$, and it was found that they very nearly coincided with the theoretical duration of the phases. The actual time available for discharge was a few percent longer than that determined by theoretical calculation. Since this would determine the final pressure in the tube after discharge, and since it meant that this pressure was lower than that required in the tube to initiate scavenging, it was felt that this would not be detrimental to the cycle of operation. At the same time, this simplified the valve timing considerably. The time available for burning, of course, varied with the valve speed, but, since the time required for burning was only an assumption, it was felt that the variation with Mach Number could be tolerated until more definite experimental results proved otherwise. Therefore, the physical valve configuration remained the same, while only the valve speed varied in accordance to the time of arrival of the interface of the new mixture to the exhaust valve and the pulse compression wave. (See Figures 5 to 9). Since these wave speeds depend on the velocity of sound of the incoming air, then the rotational speed of the valve depends only on the square root of the inlet total temperature.

The wave diagrams shown on Figures 5 to 8 were computed from the conditions of the incoming air and the tube lengths, using the method described above. Figure 9 shows the valve timing diagrams which give the angular dimensions of the open and closed portions.

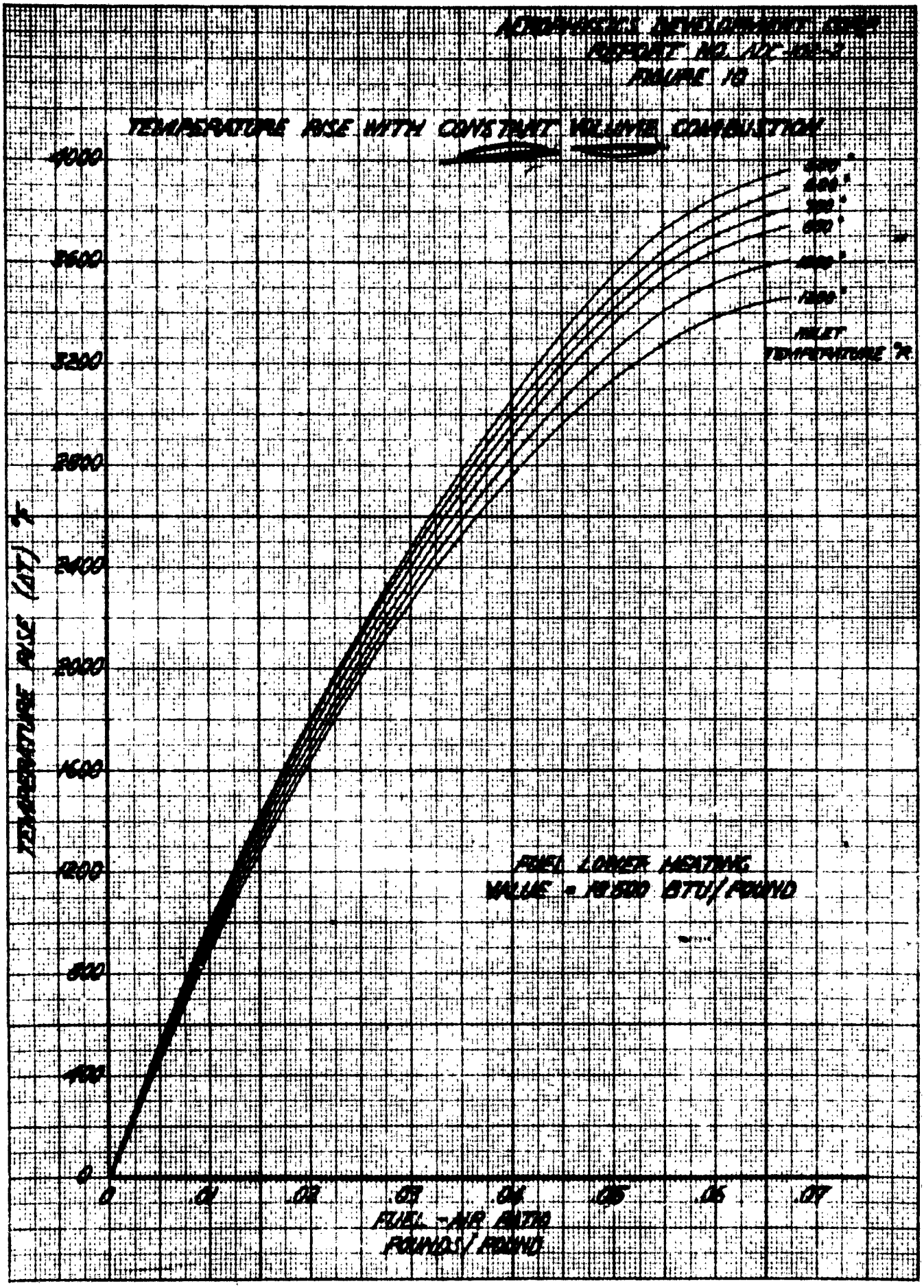
TEMPERATURE RISE WITH CONSTANT VOLUME COMBUSTION
TEMPERATURE RISE (ΔT) °F
0
400
800
1200
1600
2000
2400
2800
3200
3600
4000
0
.01
.02
.03
.04
.05
.06
.07
FUEL - AIR RATIO
POUNDS / POUND
FUEL LOWER HEATING
VALUE = 18500 BTU / POUND
INLET
TEMPERATURE °F

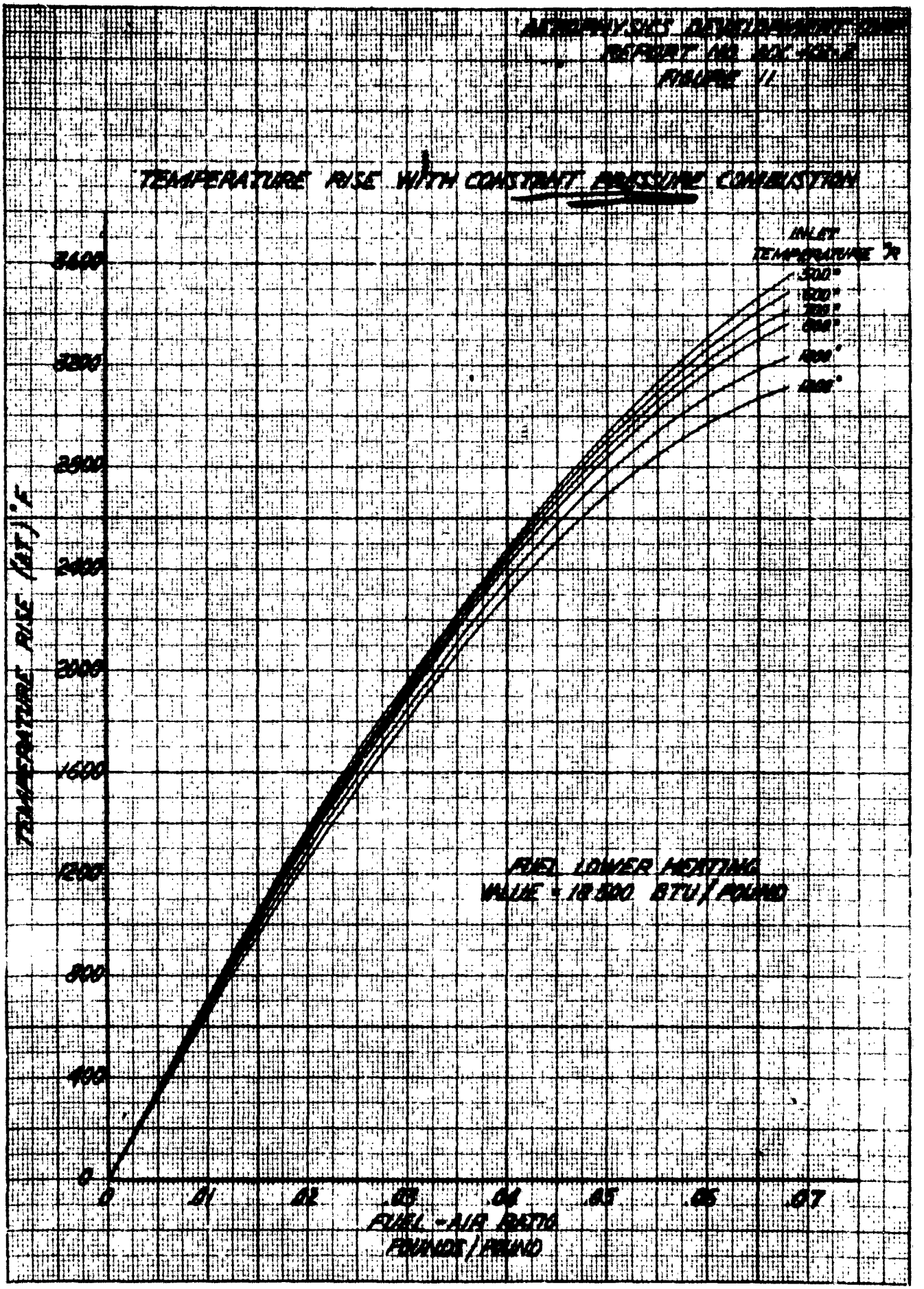
TEMPERATURE RISE WITH CONSTANT PRESSURE COMBUSTION
INLET TEMPERATURE °R
FUEL LOWER HEATING VALUE = 18 500 BTU / POUND
TEMPERATURE RISE (ΔT) °F
3400
3200
2800
2400
2000
1600
1200
800
400
0
.01
.02
.03
.04
.05
.06
.07
FUEL - AIR RATIO POUNDS / POUND

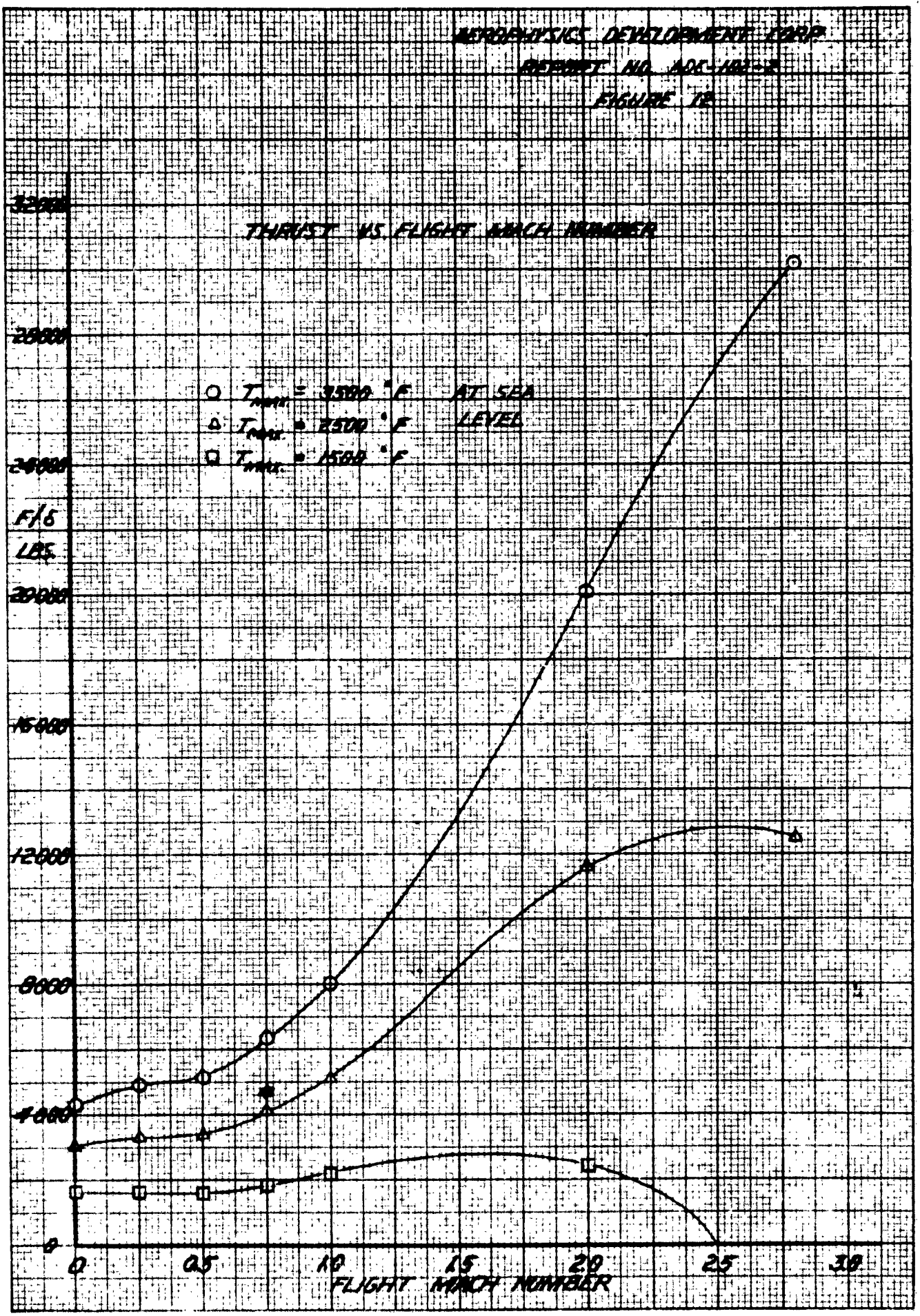
AERODYNAMICS DEVELOPMENT CORP.
REPORT NO. ADC-1001-R
FIGURE 12
THRUST VS. FLIGHT MACH NUMBER
○ $T_{max.}$ = 3500 °F AT SEA LEVEL
△ $T_{max.}$ = 2500 °F
□ $T_{max.}$ = 1500 °F
32000
28000
24000
20000
16000
12000
8000
4000
0
F/6
LBS.
0
0.5
1.0
1.5
2.0
2.5
3.0
FLIGHT MACH NUMBER

AEROPHYSICS DEVELOPMENT CORP.
REPORT NO. ADC-102-2
FIGURE 13

f - SPECIFIC FUEL CONSUMPTION
LBS FUEL / HR. PER LB THRUST

○ T_{inlet} = 3500 °F AT SEA
△ T_{inlet} = 2500 °F LEVEL
□ T_{inlet} = 1500 °F

$\frac{f}{\theta}$

3.40
3.00
2.60
2.20
1.80
1.40
1.00

0 1.00 2.00 3.00

FLIGHT MACH NUMBER

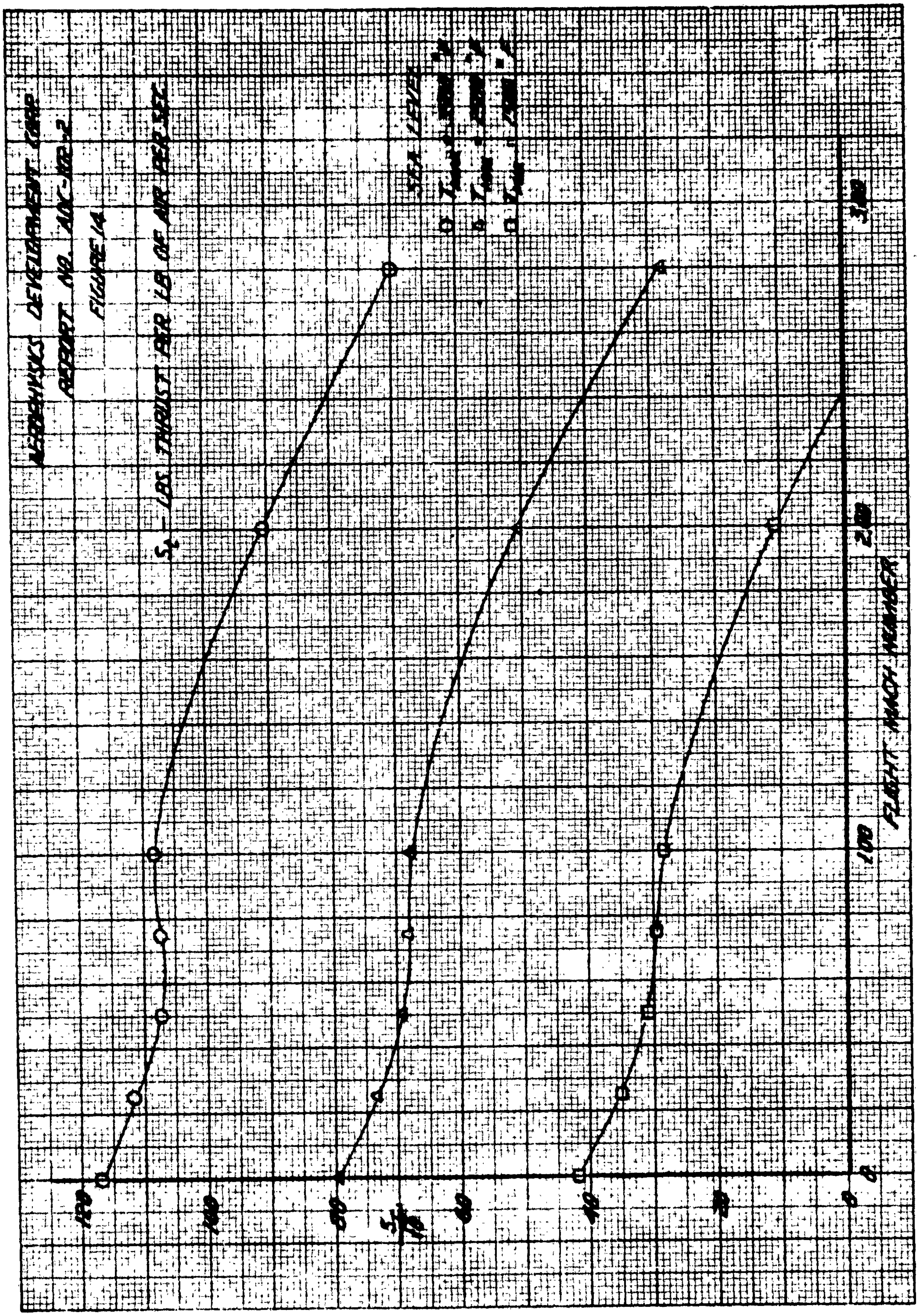
AEROPHYSICS DEVELOPMENT CORP
FIGURE 14
SEA LEVEL
LBS THRUST PER LB OF AIR PER SEC
FLIGHT MACH NUMBER
120
100
80
60
40
20
0
1.00
2.00
3.00

AEROPHYSICS DEVELOPMENT CORP.
REPORT NO. ADC-102-2
FIGURE 15

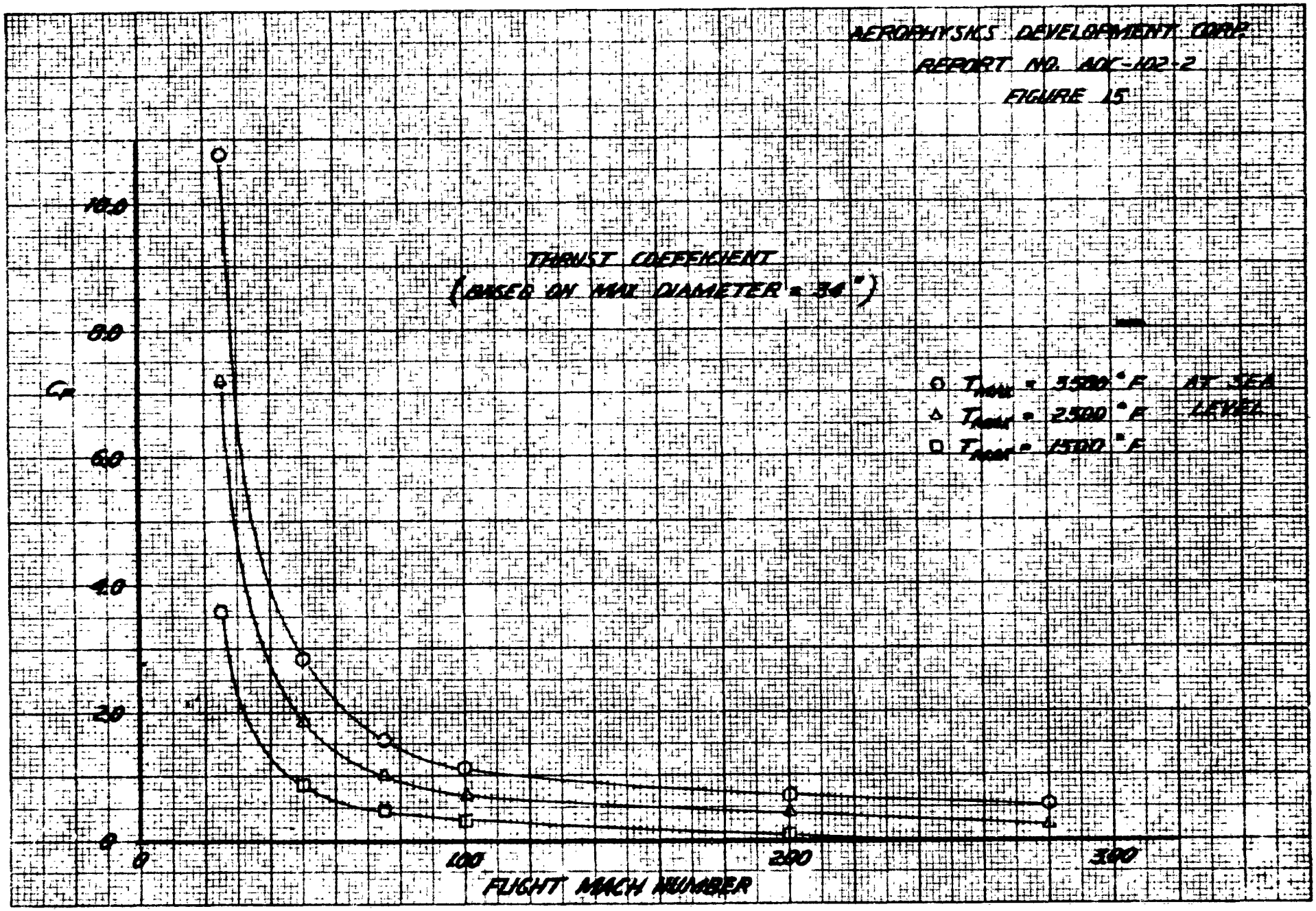

2.4 Performance Analysis of Engine

The duration of the cycle for each flight velocity was taken from the wave diagrams (Figures 5 - 8). The velocity and pressure of the scavenged burnt gases was computed and the impulse obtained from this discharge was added to make up the gross impulse produced by the engine. The intake impulse was subtracted to give the net impulse produced. The thrust was obtained by dividing the net impulse by the durations of the cycle obtained above. In calculating the thrust, the following assumptions were made regarding diffuser efficiency:

Total Pressure Ratio	Speed
1.00	$0 < M_o < 1.0$
.95	$M_o = 2$
.65	$M_o = 2.80$

A smooth curve was assumed between $M_o = 1$ and 2.80

The specific fuel consumption was computed by means of Figure 10. The difference between constant volume burning and constant pressure burning can be seen by comparing Figures 10 and 11. For the same fuel ratios, there is a smaller temperature rise for the constant pressure curves than there is for the constant volume curves. Both of these curves were computed from the data given in the tables and charts in References 3 and 4. The effect of dissociation at the higher temperatures is considered in these curves.

The performance curves were calculated for three maximum cycle temperatures (corrected for altitude): $T_{max} = 1960^{\circ}R$, $2960^{\circ}R$ and $3960^{\circ}R$. The actual maximum cycle temperature at any altitude can be found from the appropriate value of θ at that altitude. Figure 16 gives a table of the actual temperatures for various altitudes for each of the above corrected temperatures.

The maximum design pressure differential between the outside and the inside of the tubes is 500 psi (See Section III). This maximum design pressure was reduced by a factor of 1.80 in order to take care of the instantaneous local high pressure that is present immediately behind a detonation wave. In computing the design pressure differential for the tubes, it was assumed that the maximum cycle temperatures remained below $4500^{\circ}F$. The ambient pressure is equal to the ram pressure for each flight Mach Number. The maximum Mach Number for each altitude was computed and plotted on Figure 18, taking into account the above pressure and temperature limitations.

The drag coefficient of a typical large missile is plotted on Figure 17(a). The missile has a ground launch weight of 52,000 pounds, with a wing area of 425 square feet. Figure 15

AEROPHYSICS DEVELOPMENT CORPORATION ABC-102-R

PROJECT PACIFIC PALISADES, CALIFORNIA DATE

FIGURE 16

THRUST AND DRAG COEFFICIENTS

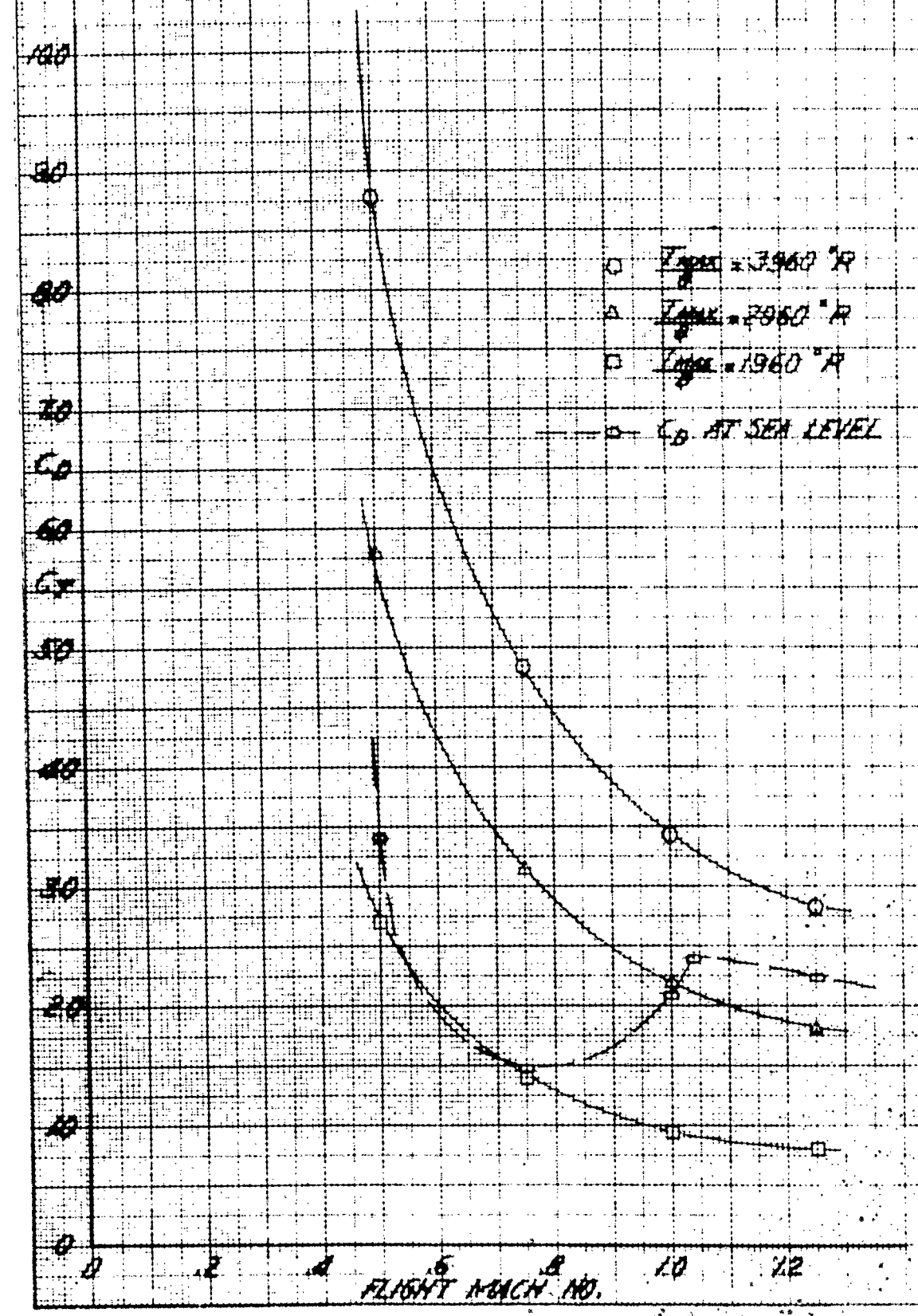

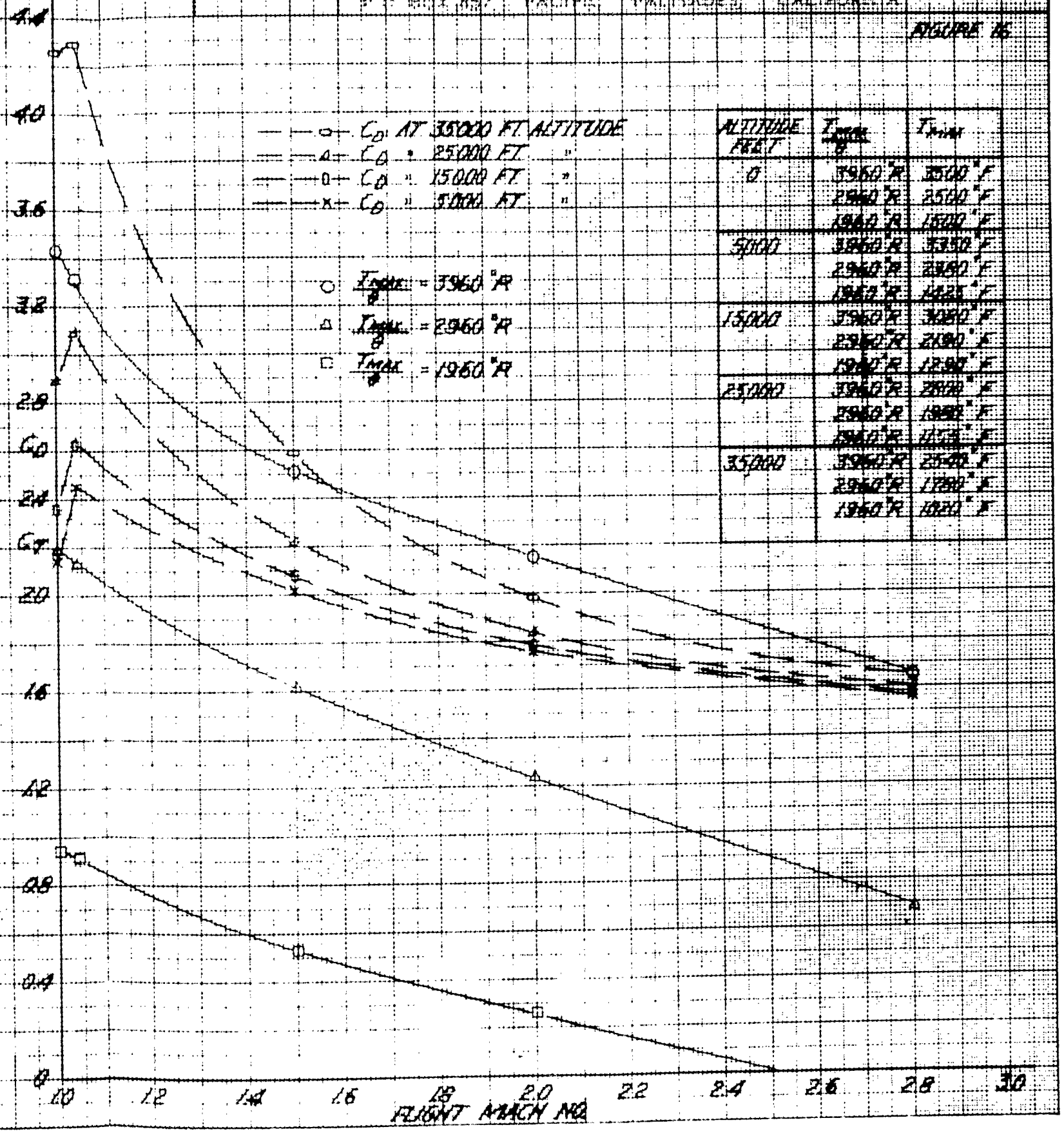

ALTITUDE FEET	$\frac{T_{max}}{\theta}$	T_{max}
0	3960 °R	3500 °F
	2960 °R	2500 °F
	1960 °R	1500 °F
5000	3960 °R	3350 °F
	2960 °R	2350 °F
	1960 °R	1425 °F
15000	3960 °R	3050 °F
	2960 °R	2100 °F
	1960 °R	1250 °F
25000	3960 °R	2900 °F
	2960 °R	1950 °F
	1960 °R	1175 °F
35000	3960 °R	2500 °F
	2960 °R	1700 °F
	1960 °R	1020 °F

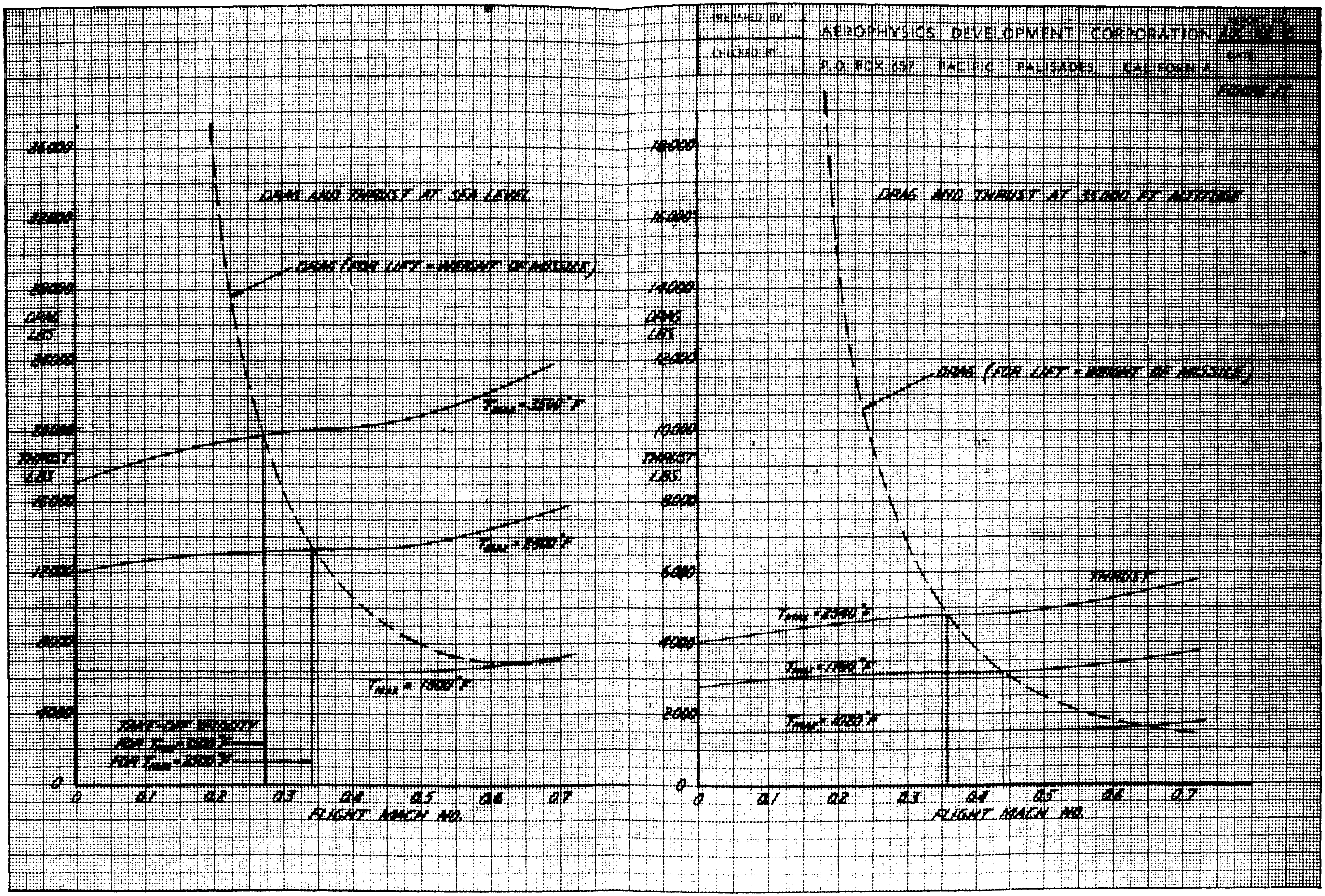
PREPARED BY
CHECKED BY
AEROPHYSICS DEVELOPMENT CORPORATION
P.O. BOX 657 PACIFIC PALISADES CALIFORNIA
DRAG AND THRUST AT SEA LEVEL
DRAG (FOR LIFT = WEIGHT OF MISSILE)
DRAG LBS.
THRUST LBS.
T_{max} = 3500°F
T_{max} = 2500°F
T_{max} = 1500°F
TAKE-OFF VELOCITY
FOR T_{max} = 1500°F
FOR T_{max} = 2500°F
FLIGHT MACH NO.
DRAG AND THRUST AT 35000 FT ALTITUDE
DRAG (FOR LIFT = WEIGHT OF MISSILE)
THRUST
18000
16000
14000
12000
10000
8000
6000
4000
2000
0
0.1
0.2
0.3
0.4
0.5
0.6
0.7

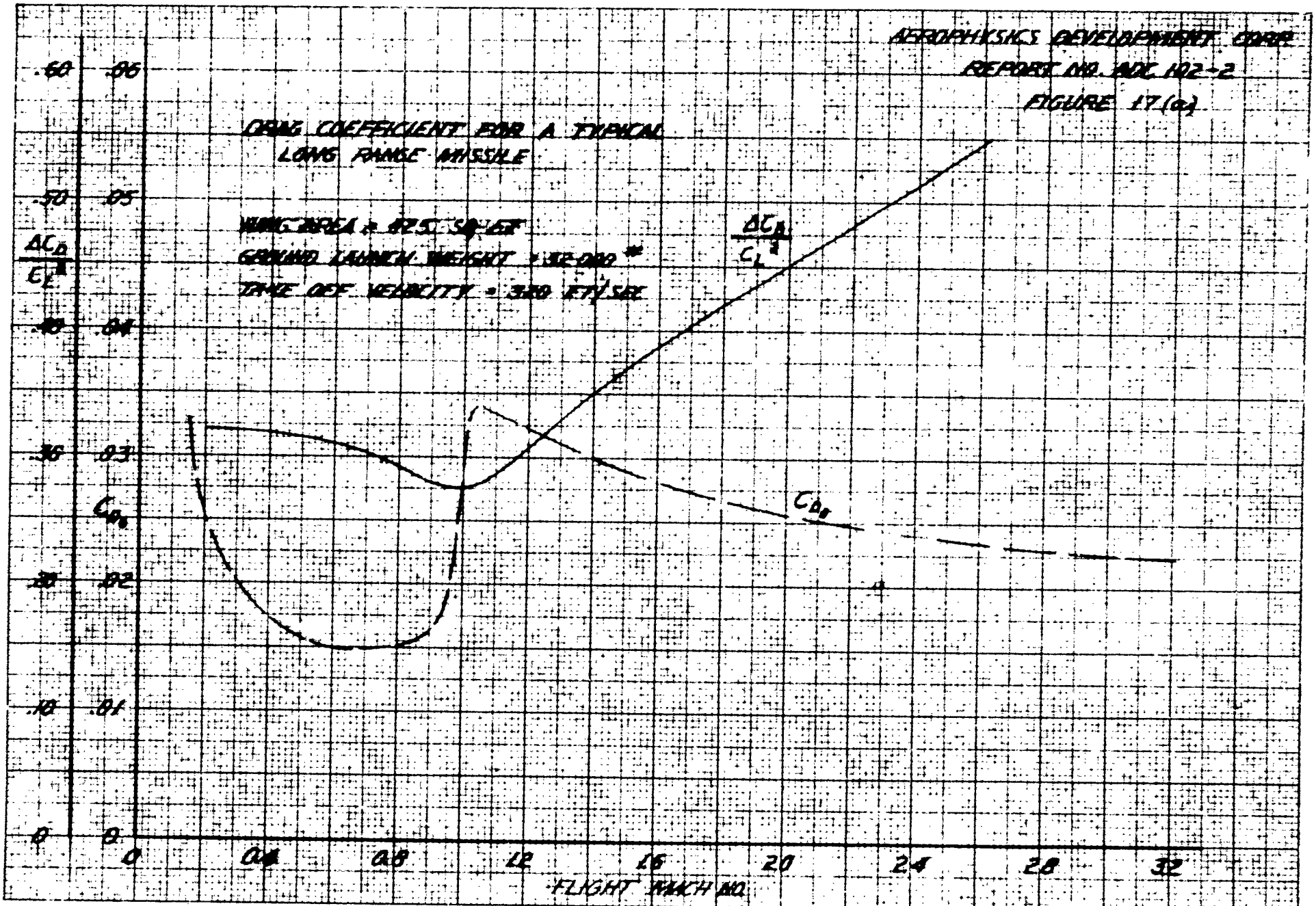

RESTRICTED

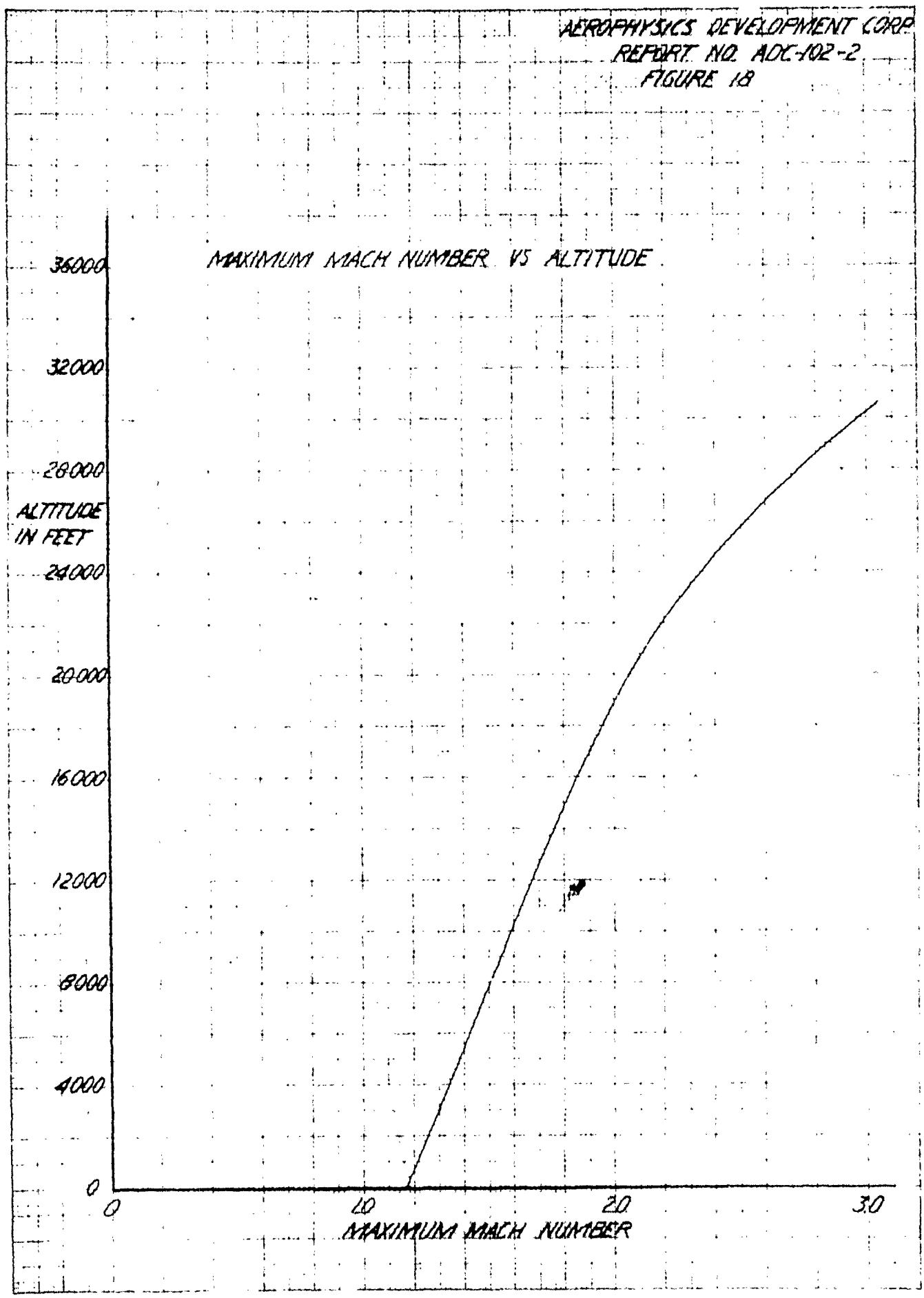
AEROPHYSICS DEVELOPMENT CORP.
REPORT NO. ADC-102-2
FIGURE 18
MAXIMUM MACH NUMBER VS ALTITUDE
36000
32000
28000
ALTITUDE IN FEET
24000
20000
16000
12000
8000
4000
0
0
1.0
2.0
3.0
MAXIMUM MACH NUMBER

shows the variation of thrust coefficient of a pulse-det-jet engine of 34-inch diameter. This engine could be scaled up or down in size but, for simplicity's sake, let us consider the performance attainable with four of these 34-inch engines weighing a total of about 3600 pounds. This powerplant weight is about half that of turbo-jets with afterburner having the same thrust at high supersonic speeds. It will be noted (Figure 16) that this system has sufficient excess thrust to accelerate through M = 1 at sea level by operating at a maximum cycle temperature T_{max} = 3000°F. The maximum cruising speed at h = 35,000 ft. will be M = 2.80 for T_{max} = 2540°. Similarly, at 25,000 feet altitude, this system has sufficient thrust to accelerate through M = 1 and accelerate to M = 2.80 by operating at T_{max} = 2800°F. From Figure 17 it will be noted that the minimum flight velocity at sea level occurs at M_{∞} = 0.27 for T_{max} = 3500°F or M_{∞} = 0.32 if T_{max} = 2500°F. Essentially, the engine is a self-accelerating ram-jet with a specific fuel consumption of 1.8 to 2.0 at the high supersonic velocities.

The maximum cross-sectional diameter of the engine is 34 inches, the length is 55 inches. The cross-sectional area of the combustion tubes is 441 square inches or 51.5% of the maximum cross-sectional area of the engine. The maximum cross-sectional area of the engine is 6.30 square feet. There are six concentric rows of 32 tubes each. The diameters of the tubes are 2.45", 2.075", 1.75", 1.40", 1.15", 0.95" from the outer to the inner rows respectively. The length of the tubes are 15". The total dry weight of the engine is approximately 900 lbs.

2.5 Leakage Losses

The leakage losses at the exhaust valve will be relatively small. The only time the exhaust valve is closed is during the pulse compression phase and during burning. During the compression phase, the pressure is low in the tubes and, therefore, very little leakage will occur. During the burning phase, the pressure will rise in the tubes and leakage will occur. On the other hand, if the feedback system is used by ducting the gases through a channel in the exhaust valve, the only leakage that would occur is through the outer periphery of the valve. Also, any leakage around the exhaust valve is not lost, as a collection chamber ducts all gases released by the engine to the exit nozzle to produce thrust. Thus it was assumed that the loss in thrust from this leakage is sufficiently small to be neglected.

The inlet valve is closed during the burning and discharge phases. The worst case would occur if the leakage losses were directly ducted to the outside and completely lost. Actually, there will be an interflow from one tube to another, and the only losses will occur at the outer edges of the inlet valve.

The pressure surrounding the inlet valve will be very nearly the total pressure of the incoming air. Actually, during the latter part of the discharge phase, the leakage will be reversed and air will flow into the tubes.

A hypothetical case under the worst conditions will have the following assumptions:

1. The total air lost through leakage at the inlet valve will be due to some flow during the discharge phase.

2. The leakage flow is completely lost to the atmosphere by each individual tube.

3. The leakage area will be that formed at the periphery of each tube for a valve clearance of 0.005".

4. The amount of flow loss due to leakage will be given by the amount of flow discharged at the exit multiplied by the ratio of leakage area to discharge nozzle area of each tube.

For the smallest tubes (diameter = 0.95 inches), the percentage of the discharged flow lost through leakage is

$$\frac{\text{Area of leakage}}{\text{Area of discharge}} = \frac{\pi \times 0.95 \times 0.005 \times 100}{\pi/4 \times 0.95^2} = 2.1\%$$

For the largest tubes (diameter = 2.45 inches), this loss is

$$\frac{\text{Area of leakage}}{\text{Area of discharge}} = \frac{\pi \times 2.45 \times 0.005 \times 100}{\pi/4 \times 2.45^2} = 0.84\%$$

The above figures indicate that 2.1% to 0.84% of the air discharged during the exhaust phase is lost through leakage. Since about 70% of the total air is discharged during the exhaust phase and since only the tubes at the periphery of the valve lose their air directly to the outside, the leakage losses will amount to only 1% of the total mass flow through the engine. Since the assumptions used to calculate the losses are quite conservative, it was decided that these losses could be neglected.

SECTION III

ANALYSIS OF THE DESIGN OF COMBUSTION TUBES

3.1 Tube Structures

At the present stage of the Pulse-Det-Jet engine design and development, it is not known what the necessity is for high combustion tube wall temperatures in order to minimize possible ignition lag and provide good combustion efficiency. The possibility exists that an uncooled tube structure may prove desirable in order to cause a rapid conversion of the flame ignition into a detonation combustion wave.

Possible cooled structures were analyzed simultaneously with uncooled structures to estimate comparative advantages and disadvantages and optimize the theoretical design as rapidly as possible. As volume and weight are critical and an inexpensive structural material is desirable, the field of present possible structural materials for an uncooled structure is very limited. In uncooled structures, the following materials were considered:

(1) Zirconium Boride plus Nickel (American Electro Metals Corporation)
(2) Metamic - LT - 1 (Haynes Stellite Div., Union Carbide and Carbon Corporation)
(3) Graphite - EBP (National Carbon Company)
(4) Graphitar (The United States Graphite Company)
(5) Stabilized Zirconium Oxide (The Norton Company)
(6) Silicon Carbide (The Carborundum Company)

The following materials were considered for possible use in cooled structures:

(1) SAE 4130 Heat Treated
(2) Stainless 19-9 DL
(3) Haynes Alloy No. 25 (Haynes Stellite Division)
(4) Kentanium K151A (Kennametal, Inc.)

Initial calculations were made to determine the equilibrium temperature of the uncooled tube exit considering only the flow through the tube. The local tube heat transfer coefficients were calculated, using turbulent flow heat transfer formula for tubes. (See Reference (5)).

$$h = \frac{k}{D} \frac{.0396 \left(R_e\right)^{.34}}{\frac{1}{P_r} + 1.5\, P_r^{-.66}\, R_e^{-.1} \left(1 - \frac{1}{P_r}\right)}$$

h = heat transfer coefficient = BTU/hr/sq ft/°F
k = thermal conductivity of gas = BTU/hr/ft/°F
D = tube diameter = feet

R_{e_d} = Reynolds Number of flow with respect to the tube diameter (dimensionless)

Pr = Prandtl Number of gas (local) (dimensionless)

The most recent extrapolations of thermal conductivity and viscosity of air by Keyes (See Reference 6) were used.

At a maximum combustion chamber temperature and pressure of 3000° F and 400 psi, respectively, it was found that the equilibrium tube wall temperature would be 2700° F. This high uncooled tube wall temperature results from the exhaust flow heat transfer coefficients being about twice the scavenge flow heat transfer coefficients and from the applied durations (the scavenging portion of the engine cycle amounts to only one-third the duration of the exhaust flow condition at the tube exit). The uncooled equilibrium tube wall temperature decreases along the tube from the exit to the forward end of the tube in a fashion substantially proportional to the duration of hot exhaust flow at the place involved in the tube. It was found that longitudinal heat transfer through the metal or ceramic wall could be neglected in comparison to the convective surface heat transfer. An equilibrium wall temperature only a few hundred degrees above the total inlet air temperature should exist at the forward end of the tube.

3.2 Cooled Tube Structures

The required heat transfer in an externally air cooled tube design for high Mach number low altitude operation was then calculated assuming a mean tube temperature of 1100° F and a tube material of heat treated 4130 steel. Although an average flow of only 5% of the total air flow passing through the tubes is required to absorb the required heat flow from the surface of the combustion tubes (temperature rise of only 130 degrees in this external air flow), the external surface area of the combustion tubes is far too small to transfer the required heat flow. Designs considering tube finning and special cross flows failed by a large margin to allow external air cooling of a simple metal tube to be considered (particularly in the region of the tube exits).

Regenerative fuel cooling of the 4130 tubes was then considered. The maximum allowable wall temperature is low as local fuel vaporization must be prevented. Under this condition, the required heat absorption by the fuel is about three times the amount that may be absorbed by the fuel without vaporization at reasonably high pressures(~ 350 psi). Recirculation of the fuel to an inlet air heat exchanger was not attractive on the basis of the trapped fuel and heat exchanger weights as well as the large pump requirements and general design engineering complexity.

Composite metal-ceramic structures were considered in order to reduce the required heat flow to an external cooling air flow.

A fundamental difficulty exists in the proper distribution of stresses with large changes in operating temperature. The mean expansion of the metal tube surrounding a ceramic liner could be matched (at least in theory) for one temperature profile but not for another. Enamel-type coatings appear to be temperature limited to about 1800° F top operational temperature at the present, and are consequently unsuitable in this application.

A structure containing both a cooled and uncooled portion was given some thought. As compressive strengths of many materials are much greater than their tensile strengths (particularly at high temperature), an uncooled combustion tube was considered to be externally pressurized by high pressure air contained in a surrounding metal tube. The surrounding metal tube was cooled by a small external air flow as the heat flow to the metal from the uncooled inner tube may be shown to be quite small. The buckling strength of the inner uncooled tube was computed by formulae given by R. G. Sturn (Reference 7) or S. B. Batdorf (Reference 8). Such a composite structure actually gave minimum total tube weights, but the scheme appears undesirable on the basis of the mechanical attachment complexity of pressurizing lines and difficulty of ensuring reasonable stable leakproof operation on the high pressure air. In addition, some source of high pressure air or gas is required.

Other materials considered for the proposed cooled structure present fundamentally the same problems as in the case of 4130. Since it is desired to have combustion chamber temperatures in excess of 3000° F, improvement in the material properties at 2000° F level does not mean too much in this design.

3.2 Uncooled Tube Structures - General

A combustion tube structure composed of uncooled tubes capable of taking the required pressure loads at high temperature would be most desirable. A review of the material properties of uncooled tube material follows.

Zirconium Boride plus nickel appears to be the most suitable material except that it is presently being made on only a laboratory scale. (Reference 9). However, it is oxidation-resistant at very high temperatures, has the excellent rupture strength of 100,000 psi at 2400° F, and is very thermal shock-resistant. Rupture strength represents a combined effect of compressive and tensile strengths, and it may be that the tensile strength is considerably less than the rupture strength. However, even 20,000 psi tensile strength at 2400° F would be most excellent. The thermal conductivity of Zirconium boride is in the range of the alloy steels and its density is only two-thirds that of steel. Experiments which plunge samples heated to 4710° F into water with no material fracture demonstrate its excellent thermal shock properties. More information is being sought of American Electro Metals Corporation to determine the feasibility of using Zirconium boride tubes as the combustion ducts of the Pulse-Det-Jet engine. Presently lacking

is information on its elastic modulus, expansion coefficient, specific heat, and creep strength data up to high temperatures.

Metamic becomes quite weak at elevated temperatures (LT-1 has a tensile strength of 3400 psi at about 2400° F), (See Reference 10), and the tensile strength versus temperature decreases in a fashion such that very little strength would be expected at 3000° F. In addition, the thermal and mechanical shock stability of Metamic, though better than many materials, does not appear good enough for the rigorous conditions imposed by this engine.

Graphite has excellent thermal shock properties, but is low in thermal strength and oxidizes in air above 700° F. However, graphite increases in tensile strength and in elastic modulus with an increase in temperature up to about 4500° F, (See Reference (11), (12). In addition, it is known (verbal communication) that graphite can be coated with molybdenum disilicide or silicon carbide to form a thin oxidation-resistant coating which is adherent over a wide temperature range. The molybdenum disilicide coating is less rough than the silicon carbide coating and would probably be preferable in this application. A design tensile strength of 3000 psi is considered at high temperatures for a graphite structure similar to EBP of the National Carbon Company. Such a structure appears theoretically feasible and is presently considered in the design of the Pulse-Det-Jet Engine with the possibility of Zirconium Boride tubes as an alternate tube material. The required wall thickness to diameter and length ratios are less than those easily available, but it is believed thicker pieces could be molded and turned down to the required thickness. The coatings on individual tubes and their strength could be tested before assembly and defective tubes discarded.

Graphitar is the trade name of the U.S. Graphite Company for their graphite-carbon mixtures. A wide range of material properties may be achieved, but the largest values of tensile strength are obtained on the purest graphite samples. Lower thermal conductivity may be obtained by the addition of carbon with a sacrifice in thermal strength. Graphite-carbon bodies offer no theoretical advantage for use as uncooled combustion tubes as compared to pure graphite bodies.

Stabilized Zirconium Oxide of the Norton Company (reference 13) apparently has many desirable properties for use at high temperatures, but it is highly dubious that it is sufficiently thermal shock resistant as its thermal conductivity and specific heat are low.

Silicon Carbide has an excellent thermal conductivity, but its modulus of rupture is only 800 to 3125 psi at 2460° F (Reference 14), so that thick walls must be used in such proposed combustion ducts.

AEROPHYSICS DEVELOPMENT CORP.
REPORT NO. ADC-102-2
FIGURE 19

REPRESENTATIVE TEMPERATURE AND STRESS PROFILES IN TUBE WALL

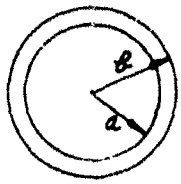

INITIAL COMBUSTION CONDITIONS AT LOW MACH NO.

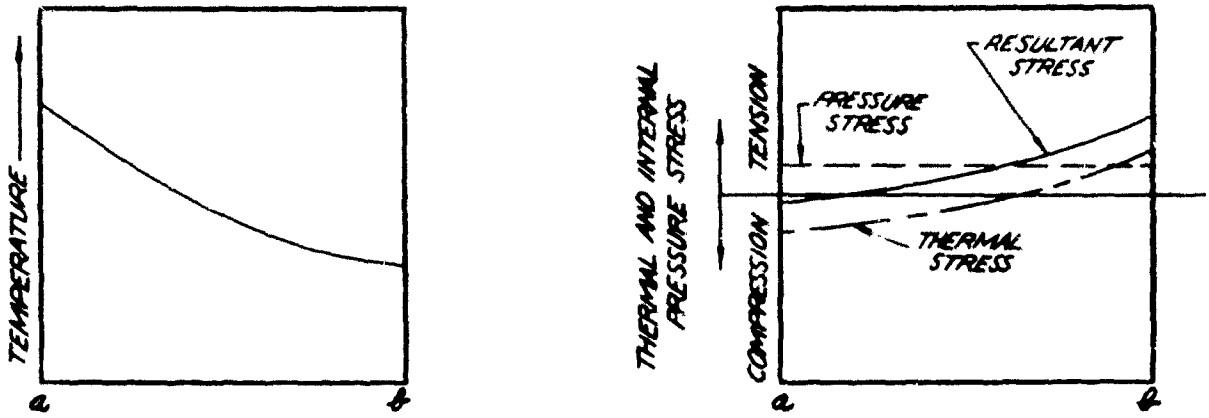

STEADY STATE COMBUSTION CONDITIONS AT HIGH MACH NO. AND LOW ALTITUDE

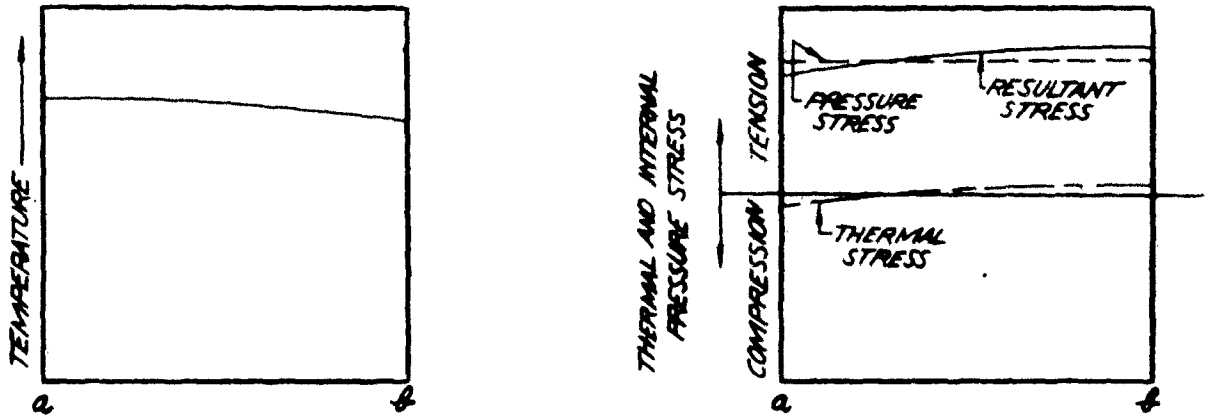

FLAME OUT AT HIGH MACH NO. AND LOW ALTITUDE

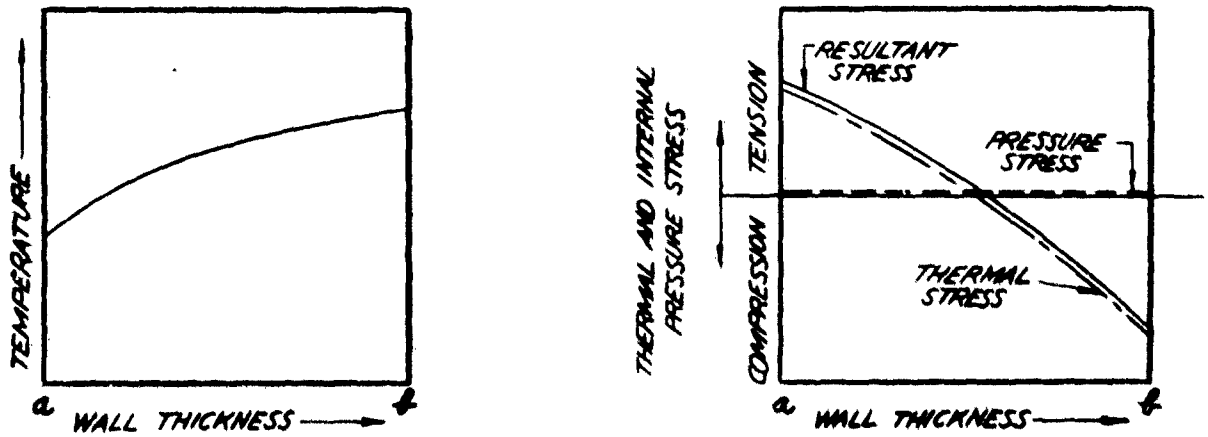

3.3 Thermal Shock Considerations

As thermal shock properties often appear to be critical in the design of the uncooled combustion tubes for the Pulse-Det-Jet engine, a review was made of existing thermal shock or stress theory. A recent article by C. M. Cheng (Reference 15) shows good correlation between theory and experiment concerning the thermal shock failure of flat plates. Timoshenko (Reference 16) gives a thermal stress analysis for tubes as well as flat plates that does not analyze in detail the temperature gradients that result as a consequence of the resistance factor ($R = k/hb$), as shown by Cheng, but formulates the thermal stress equation to allow the determination of stresses for any assumed or calculated temperature gradient. Now transient heat transfer charts (Reference 17) allow the temperature profile in a material to be determined readily so than an approximate conservative temperature difference is obtained for use in Timoshenko's formula for thin wall tubes:

$$\sigma = \frac{\alpha E \Delta T}{2(1-\upsilon)}$$

σ = thermal stress = psi

α = thermal expansion coefficient = inches/inch/^{o}F

E = Modulus of Elasticity = psi

ΔT = Temperature difference = ^{o}F

υ = Poisson's Ratio = dimensionless

The tube tensile strength at the local temperature must be greater than the thermal stress to prevent fracture.

Figure 19 gives representative temperature and stress profiles in an uncooled tube wall as determined by the flight condition. It may be perceived that the most critical thermal stress will exist in a tube wall at the cessation of combustion at the highest flight speed and lowest altitude. The thicker the tube wall, the larger may be the maximum internal tube pressure, as given by the conventional hoop stress formula for thin tubes:

$$\sigma = \frac{r P}{t}$$

σ = tensile stress = psi

r = tube radius = inches

t = tube thickness = inches

P = pressure differential across tube wall = psi

HIGH TEMPERATURE COMBUSTION TUBE MATERIAL COMPARISON

MATERIAL	COEFFICIENT OF THERMAL EXPANSION ϵ = in./in./°F	THERMAL CONDUCTIVITY k = BTU/hr/ft²/°F/in	MODULUS OF ELASTICITY E = psi	DENSITY ρ = lbs/cu.in.	POISSON'S RATIO ν	SPECIFIC HEAT C_p = BTU/lb/°F	TENSILE STRENGTH σ = psi	THERMAL DIFFUSIVITY α = ft²/hr.	REMARKS
Zirconium Boride (ZrB_2) + 5% Nickel	~5.5 x 10^{-6} at T > 1840°F for ZrB_2 only	169 @ 60°F		.161			Short time Rupture strength is 100000 psi at 2400°F		Small samples have been heated to 4710° F and plunged into water without cracking. Very oxidation resistant.
Graphite (EBP)	1.2 x 10^{-6} over wide range of temperature	1200 @ 60°F 87 @ 1800°F estimated at 40 @ 3000° F	.12 x 10^{7} @ 3000°F	.061	.35 @ 60°F	.165 Mean from 78° F to 169° F .390 Mean from 132°F to 2645° F	3500 @ 60°F 4500 @ 3000°F 6500 @ 4700°F 0 @ 5000°F Short time tests	~4.5 x 10^{-2} @ 3000°F estimated	Oxidizes above 700°F Extremely thermal shock resistant but must be coated to resist oxidation.
Stabilized Zirconium Oxide (Dense) (Norton)	~3 x 10^{-6} from 60°F to 3000° F	5.5 @ 60° F 6.2 @ 2000° F ~7.5 @ 3000° F	2.[illegible] x 10^{7} @ 1800° F	.182		.175 Mean from 75° F to 2060° F	6750 @ 1800° F Believed to be nearly this value @ 3000° F	~1.34 x 10^{-2} @ 3000° F estimated	Very low thermal conductivity at high temperatures. Somewhat sensitive to thermal shock
Silicon Carbide	4.7 x 10^{-6} @ 2460°F	109 @ 2200°F		.112		~ .2	Rupture strength is 600-3126 @ 2460° F		Oxidation resistant. Good thermal shock resistance. Low tensile strength at 3000° F.
Metamic LT-1	4.7 x 10^{-6} Mean from 32° F to 1832°F	83 Mean from 60° F to 1000° F		.1[illegible]			17500 @ 1300°F 13000 @ 2000°F 7000 @ 2200°F 3[illegible]00 @ 2400°F Short time		M.P. = 3362° F, so strength @ 3000° F is probably low. Somewhat sensitive to thermal shock
[illegible] K151A [illegible] + 20% Ni	4.5 x 10^{-6} up to 1200°F	240 @ 60° F	5.67 x 10^{7}	.21	Note: ν varies little from .[illegible] for most materials	Note: C_p varies little from .3 for most materials	40000 @ 2000° F Short time test 10500 @ 1800[?]° F for stress rupture at 10 hours.		Good material at 2000° F, but probably has little strength at 3000° F.

AEROPHYSICS LEVELOPMENT CORP.
REPORT NO. ADC-102-2

HIGH TEMPERATURE COMBUSTION TUBE MATERIAL COMPARISON FIGURE 21

MATERIAL	DESIGN TENSILE STRENGTH ASSUMED AT 3000° F psi	AT 400 psi PRESSURE WALL THICKNESS OF 275" I.D. TUBE (S)	ESTIMATED FOURIER NUMBER FOR t = .01 hrs. $f = \frac{\alpha t}{s^2}$	ESTIMATED THERMAL RESISTANCE NUMBER R = 1/bs	CALCULATED STRESS UPON COOLING FROM 3000° F (STEADY FLOW) psi
Zirconium Boride (ZrB_2) + 5% Nickel	15000	.0367"	45.6	5.74	19000
Graphite (EBP)	3000	.1833"	1.9	1.09	1100
Stabilized Zirconium Oxide (Dense) Norton	5000	.110"	1.6	.359	78000

RESTRICTED

RESTRICTED

However, the thicker the tube wall, the greater will be the temperature difference, ΔT, upon starting and stopping combustion with resulting greater thermal stresses. Upon cessation of combustion in an uncooled tube, the outer tube fibers at high temperature are put into compression as the inner tube fibers seek to contract upon cooling and are prevented because of adherence to the outer tube fibers. Thus the inner tube fibers are put into tension at an initially high temperature. Upon heating the tubes initially by the combustion, the inner tube fibers are put into compression, the initially cold outer tube fibers in tension. The difference in the material temperature level should make the cessation of combustion case the most critical.

Figure 20 summarizes available information on various high temperature materials. It is obvious that more information is required to accurately evaluate combustion tube material on a theoretical basis as to thermal stressing. However, using this information and making educated guesses of the unknown quantities, the calculation of approximate required tube thickness and thermal stress as a stringent cooling requirement is allowed. The results of these calculations are presented in Figure 21. Charts for transient heat transfer in flat plates were used to determine the maximum thermal stress in the tube wall. (See Reference 17). For the present wall thickness to diameter ratios used, this is a good approximation. The temperature profile versus radius was then plotted and the temperature difference obtained. Timoshenko's formula was then used to obtain the maximum stresses (Reference 16). It is believed that the calculations are conservative, even by a factor of two, as some material variations in specific heat and thermal conductivity with temperature have been neglected as well as the easing of local temperature gradients caused by preheating of boundary layer air by the preceeding tube areas and an intermittent air flow (flow occurs only 50% of the time, whereas steady state flow has been assumed in the thermal stress calculation). From Figure 18, it is perceived that only graphite or Zirconium Boride plus nickel may be considered in this application on the basis of the thermal shock calculations. Thermal shock calculations for silicon carbide, Metamic LT-1, and Kentanium K-151A were not made, as their properties at 3000° F are not sufficiently good to warrant serious consideration.

FIG. 22

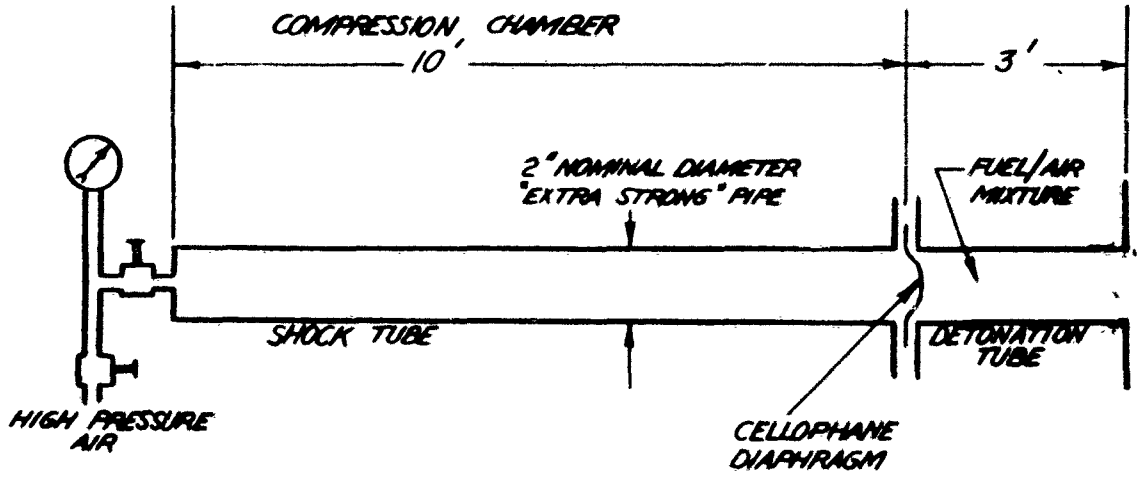

LAYOUT OF PRESENT SHOCK TUBE FOR DETONATION EXPERIMENTS

RESTRICTED

SECTION IV

EXPERIMENTS ON DETONATION

4.1 Experimental Apparatus

A shock tube has been set up in which the detonation of fuel/air mixtures by means of shock waves can be investigated. A simple layout sketch of the apparatus is shown in Figure 22. This tube is enclosed in a 4-inch pipe casing for safety precautions. The right end of the detonation tube is left open and a window in the 4-inch casing makes it possible to observe the open end of the detonation tube. Pressures up to 100 psi gage have been used in the compression chamber. With this pressure, when the cellophane diaphragm breaks, a shock wave having a pressure ratio of 2.40 is propogated through the detonation tube. The detonation tube is filled with the fuel/air mixture and the observation of a flash at the open end of the detonation tube will indicate that a detonation wave has been initiated by the shock wave.

The results of these experiments will be reported in the next progress letter.

BIBLIOGRAPHY

1. Bitondo, D. Preliminary Performance Analysis of the Pulse-Detonation-Jet Engine System. Report No. ADC-102-1, Aerophysics Development Corporation, Pacific Palisades, California, April, 1952.

2. Gunderley, G. Nonstationary Gas Flow in Thin Pipes of Variable Cross Section. National Advisory Committee for Aeronautics, T-M 1196, December, 1948.

3. Hottel, H.C.; Williams, G.C.; Satterfield, C.N. Thermodynamic Charts for Combustion Processes. First Edition, Parts One and Two, John Wiley and Sons, Inc., New York, 1949.

4. Keenan, J.H.; Kaye, J. Gas Tables. John Wiley and Sons, Inc., New York, 1948. pp. 38-98.

5. Eckert, E.R.G. Introduction to the Transfer of Heat and Mass. First Edition. McGraw-Hill Book Company, Inc., New York, 1950, p. 113.

6. Keyes, F.G. "A Summary of Viscosity and Heat Conduction Data for He, A, H_2, O_2, N_2, CO, CO_2, H_2O, and Air". "Measurements of the Heat Conductivity of Nitrogen-Carbon Dioxide Mixtures". Trans. ASME, July, 1951, Vol. 73 No. 5, p. 589-605.

7. Sturm, R.G. A Study of the Collapsing Pressure of Thin-Walled Cylinders, University of Illinois Bulletin, Vol. 39, No. 12, Nov. 11, 1941.

8. Batdorf, S.B. A Simplified Method of Elastic Stability Analysis for Thin Cylindrical Shells, National Advisory Committee for Aeronautics Report No. 874, 1947

9. American Electro Metals Corporation Summary Report, Cemented Borides, American Electro Metals Corp., Yonkers New York, Feb. 1, 1949 - Dec. 1, 1950 (Restricted)

10. Haynes Stellite Div., Union Carbide and Carbon Corp., New York, Refractic Metal Ceramics, F-7480, P-8646l.

11. Malmstrom, C.; Keen, R.; Green, L., Jr. Some Mechanical Properties of Graphite at Elevated Temperatures, Jour. of Applied Physics, Vol. 22, No. 5, May, 1951, pp. 593 - 600.

12. Green, L., Jr. The Behavior of Graphite Under Alternating Stress, ASME Paper No. 51, APM-3, Feb. 6, 1951.

13. Norton Company Technical Bulletin, Norton Fused Stabilized Zirconia, Norton Co., Worcester, Massachusetts.

14. Carborundum Co., Refractories Division, Niagara Falls, N.Y., Carbofrax.

15. Cheng, C. M. Resistance to Thermal Shock, Jour. of the American Rocket Society, Vol. 21, No. 6, Nov. 1951, pp. 147 - 153.

16. Timoshenko, S. & Goodier, J.N. Theory of Elasticity, McGraw-Hill Book Company, Inc., Second Edition, 1951, pp. 412, 415.

17. Jakob, Max Heat Transfer, Vol. I, John Wiley & Sons, Inc., New York, 1950. pp. 285, 288.